LOADING OF DOXORUBICIN INTO LIPOSOMES BY FORMING Mn^{2+}-DRUG COMPLEXES

by

CHUNG-LING CHEUNG

B.Sc. (Honours), The University of Calgary, 1996

A THESIS SUBMITTED IN PARTIAL FULFILLMENT OF
THE REQUIREMENTS FOR THE DEGREE OF

MASTER OF SCIENCE

in

THE FACULTY OF GRADUATE STUDIES

(Department of Biochemistry and Molecular biology)

We accept this thesis as conforming
to the required standard

THE UNIVERSITY OF BRITISH COLUMBIA

June 1998

In presenting this thesis in partial fulfilment of the requirements for an advanced degree at the University of British Columbia, I agree that the Library shall make it freely available for reference and study. I further agree that permission for extensive copying of this thesis for scholarly purposes may be granted by the head of my department or by his or her representatives. It is understood that copying or publication of this thesis for financial gain shall not be allowed without my written permission.

Department of Biochemistry and Molecular Biology

The University of British Columbia
Vancouver, Canada

Date June 30, 98

Abstract

Doxorubicin has been encapsulated into liposomes with a transmembrane pH gradient. In this thesis, a new procedure for loading doxorubicin into large unilamellar vesicles (LUVs) is characterized and compared to loading using the ionophore A23187 with $MnSO_4$-containing liposomes. It is shown that doxorubicin can be loaded into LUVs composed of sphingomyelin/cholesterol (55/45 mole/mole) in response to a transmembrane $MnSO_4$ gradient in the absence of a transmembrane pH gradient. Complex formation between doxorubicin and Mn^{2+} is found to be a driving force for doxorubicin uptake. Uptake levels approaching 100 % can be achieved up to a drug-to-lipid molar ratio of 0.5 utilizing an encapsulated $MnSO_4$ concentration of 0.30 M. *In vitro* leakage assays show excellent retention properties over a 24 hour period. The possible advantages of a liposomal formulation of doxorubicin loaded in response to entrapped $MnSO_4$ are discussed.

Table of Contents

List of Tables

List of Figures

Abbreviations

A_C: cross sectional area of fatty acyl chains

A_H: cross sectional area of lipid headgroup

H_{II}: hexagonal phase

^{3}H-CHE: ^{3}H-Cholesteryl hexadecyl ether

i.v.: intravenous

LUVs: large unilamellar vesicles

MLVs: multilamellar vesicles

PA: phosphatidic acid

PC: phosphatidylcholine

PE: phosphatidylethanolamine

PG: phosphatidylglycerol

ΔpH: pH gradient

pH_i: intraliposomal pH

pH_o: extraliposomal pH

PI: phosphatidylinositol

pK_a: -log acid ionization constant

pK_D: -log dissociation constant

PS: phosphatidylserine

SUVs: small unilamellar vesicles

T_m: mid-point phase transition temperature

v/v: volume-to-volume ratio

Acknowledgements

Acknowledgement.... or express appreciation of.... I find this section in every book I have read and all seminars I have attended. Every author or presenter gives a long list of names, an incredibly long list, to readers or audiences who enjoy sharing the appreciation for the contributions they have made. But among them, there are a few who could not care less about any of them. During my two-year stay at the University of British Columbia, I have met a lot of incredibly nice people who provided me with tremendous help. So I want to take this opportunity to acknowledge their contributions and hope those readers (if any!) would take a minute to share my appreciation toward them.

First of all, I would like to sincerely thank Dr. Pieter R. Cullis, my supervisor, for giving me the opportunity to work, learn, and enjoy life in his laboratory. I am also grateful for Dr. M. Bally and Dr. R. Molday's participation in my graduate committee and their invaluable advice. In addition, I am thankful for everyone whom I have worked with in the laboratory (in alphabetical order): Allison, Angel, Conrad, Dave, Dora, Elisabeth, Ismail, Ken, Kim, Lenore, Lorne, Norbert, and especially *Hanneke Leenhouts* and *Tyler Sun* for their guidance and inputs in my project.

I also want to thank NSERC for providing me a graduate studentship, MRC of Canada for funding this project, Dr. Trip for giving me the opportunity to work as a T.A., Sharon Krowchuk for her assistance in the department, Gary, Emily, and Thuan for their company in the everlasting graduate laboratory course, and last but not least, Dr. R. Barton for teaching me three very interesting courses in the graduate program.

Dedication

This thesis is dedicated to:

King, my father

May, my mother

and my sister ***Rita***

Chapter 1
Lipids and Doxorubicin

1.1 Introduction

1.1.1 Background information on phospholipids

Biological membranes play an important role in all living cells. Its semi-fluidity and selective permeability are unique properties that allow membranes to constrain cellular constituents. These qualities originate from the amphipathic nature of phospholipid molecules. As illustrated in Figure 1, the polar region of all phospholipids is comprised of the headgroups, and the nonpolar characteristics originate from the fatty acyl chains.

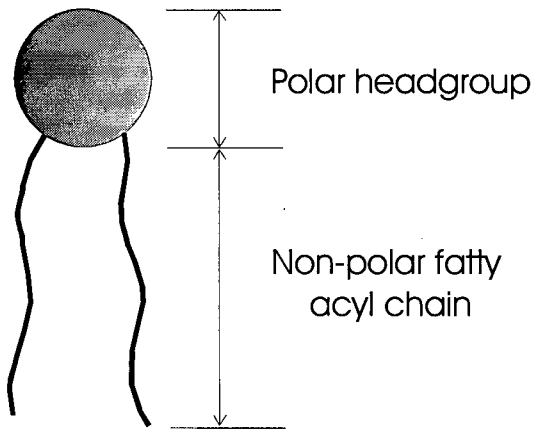

Figure 1. Schematic representation of a phospholipid molecule

Phospholipids can be composed of a huge variety of headgroups and fatty acyl chains. Figure 2 summarizes the common phospholipid headgroups found in cell membranes: phosphatidic acid (PA), phosphatidylcholine (PC), phosphatidylethanolamine (PE), phosphatidylserine (PS), phosphatidylglycerol (PG), phosphatidylinositol (PI), cardiolipin, and sphingomyelin. These headgroups can be attached to various fatty acyl chains, which vary in length and degree of unsaturation, to give membranes a wide range of properties. Some common examples of acyl chains are illustrated in Table 1. Both the headgroups and the acyl chains play a critical role in determining the morphology, fluidity, transition temperature, and function of membranes.

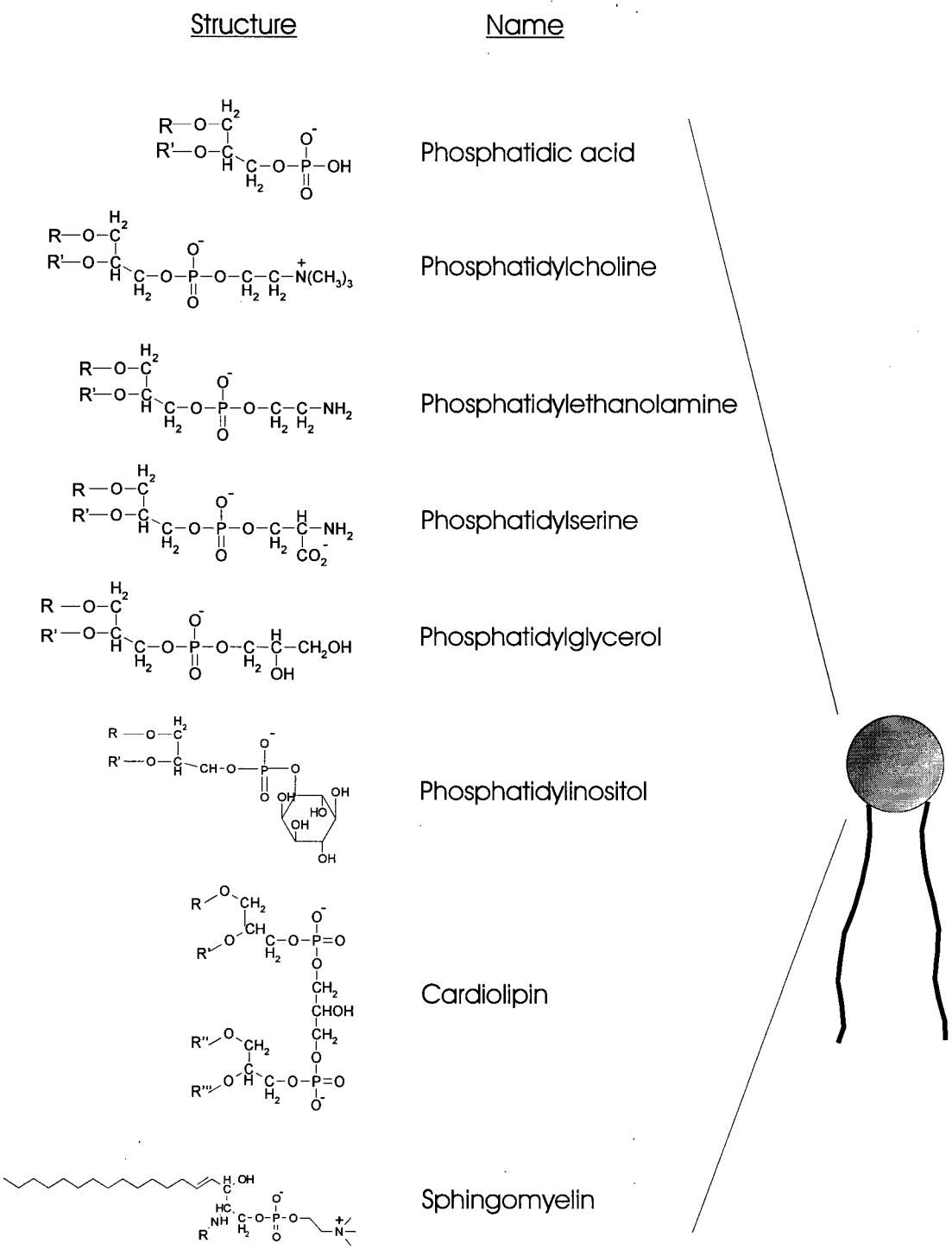

Figure 2. Structures of common phospholipid headgroups

Table 1. Structures of common saturated and unsaturated fatty acids

Saturated fatty acids

Lauric acid	CH_3-$(CH_2)_{10}$-COOH
Myristic acid	CH_3-$(CH_2)_{12}$-COOH
Palmitic acid	CH_3-$(CH_2)_{14}$-COOH
Stearic acid	CH_3-$(CH_2)_{16}$-COOH
Arachidic	CH_3-$(CH_2)_{18}$-COOH
Behenic	CH_3-$(CH_2)_{20}$-COOH

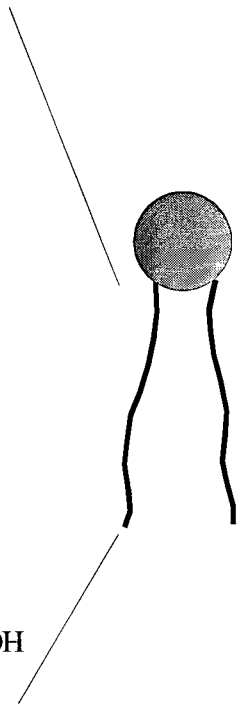

Unsaturated fatty acids

Monounsaturated (all cis-double bonds):

Palmitoleic acid	CH_3-$(CH_2)_5CH=CH(CH_2)_7$-COOH
Oleic acid	CH_3-$(CH_2)_7CH=CH(CH_2)_7$-COOH
Vaccenic acid	CH_3-$(CH_2)_5CH=CH(CH_2)_9$-COOH

Polyunsaturated (all cis-double bonds):

Linoleic acid	CH_3-$(CH_2)_4CH=CHCH_2CH=CH(CH_2)_7$-COOH
Linolenic acid	CH_3-$CH_2CH=CHCH_2CH=CHCH_2CH=CH(CH_2)_7$-COOH
Arachidonic acid	CH_3-$(CH_2)_4(CH=CHCH_2)_3CH=CH(CH_2)_3$-COOH

1.1.2 Lipid polymorphism

In aqueous environment, lipid aggregates can adopt various morphological structures. Depending on the molecular geometry, lipids can form micelles, bilayers or the hexagonal (H_{II}) structures (Cullis et al., 1983). The ratio between the cross sectional area of the headgroup (A_H) and the fatty acyl chains (A_c) is a very important parameter in determining the geometry of lipid molecules.

(i) Micelle-forming lipids:

Lipid molecules with a large ratio of headgroup-to-acyl chain cross sectional area (>1) exhibit an inverted conical geometry (Figure 3A). Lysolipid (lipid with only one hydrocarbon acyl chain) and detergent molecules have shapes resembling an inverted cone, and they adopt the micelle morphology in aqueous solutions.

(ii) Bilayer-forming lipids:

Lipids with a uniform headgroup-to-acyl chain cross sectional area ratio (from 0.5 to 1) are cylindrical in shape (Figure 3B). Their aggregates spontaneously adopt the bilayer morphology in aqueous environment. PA, PC, PG, PI, PS, cardiolipin, sphingomyelin, and digalactosyldiglyceride are examples of bilayer-forming lipids.

(iii) H_{II}-forming lipids:

Lipids which possess a small headgroup-to-acyl chain cross sectional area ratio (<0.5) exhibit a conical geometry. These lipid aggregates adopt the H_{II} morphology upon hydration (Figure 3C). Unsaturated PE, cardiolipin in the presence of Ca^{2+}, PA with Ca^{2+} at pH < 6, PA without Ca^{2+} at pH < 3, monogalactosyldiglyceride, and PS below pH 4 are lipids that belong to this category.

Lipid polymorphism is highly dependent on all types of lipid molecules that are present. Due to differences in the molecular geometry, different lipids can complement each other, thus altering the overall morphology. Biological membranes are composed of a wide range of lipids, therefore lipid polymorphism is an important factor in determining the properties of different membranes.

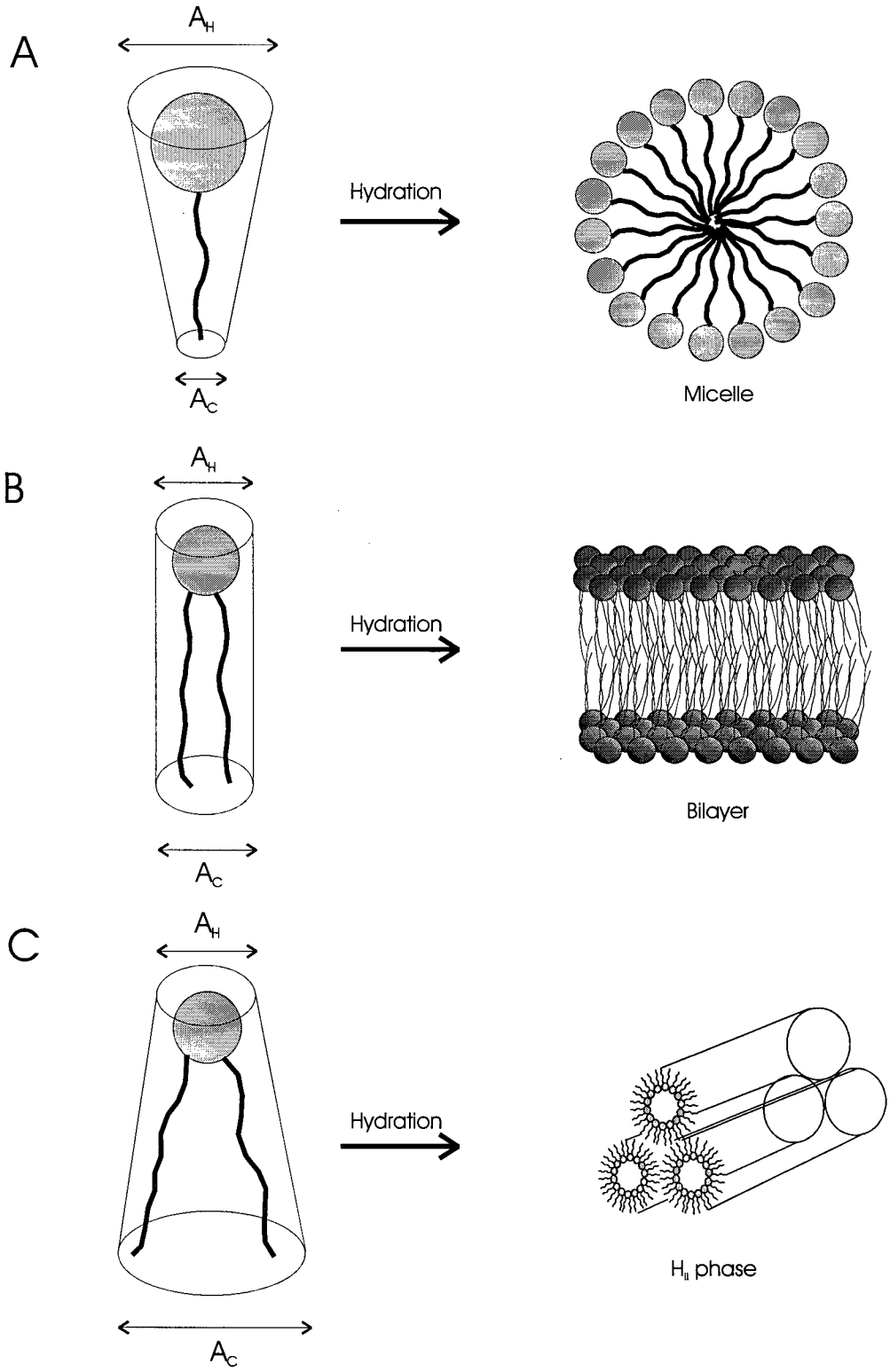

Figure 3. Molecular geometry and morphological structures of lipids

1.1.3 Transition temperature of lipids

Extensive hydrophobic interactions between fatty acyl chains minimize their contact with the aqueous environment by orienting the hydrophilic lipid headgroups toward the aqueous media. Most interactions between adjacent lipid molecules occur at the hydrophobic acyl chain region, and temperature is an important determinant in the degree of interaction between the acyl chains. At low temperature, the molecular movement of acyl chains is impeded. This causes lipid molecules to stay closer together, resulting in an increase in the van der Waals interactions between fatty acyl chains. The increased interaction leads to a rigid bilayer structure known as the gel state (Figure 4A). In the gel state, the tightly packed lipid molecules hinder the passage of molecules through the bilayer. However as temperature rises, the increase in the molecular motion between acyl chains causes lipid molecules to remain further apart. This reduces the strength of van der Waals interactions, thus resulting in an increase in the membrane fluidity. When temperature is high enough and fluidity is sufficient to allow lipid molecules freely to translocate longitudinally, membrane-permeable solutes can pass through lipid bilayers readily. This is referred to as the liquid-crystalline state (Figure 4B). During the transition between the gel and liquid-crystalline state, the temperature at which 50 % of the transition has taken place is known as the T_m, or the mid-point transition temperature.

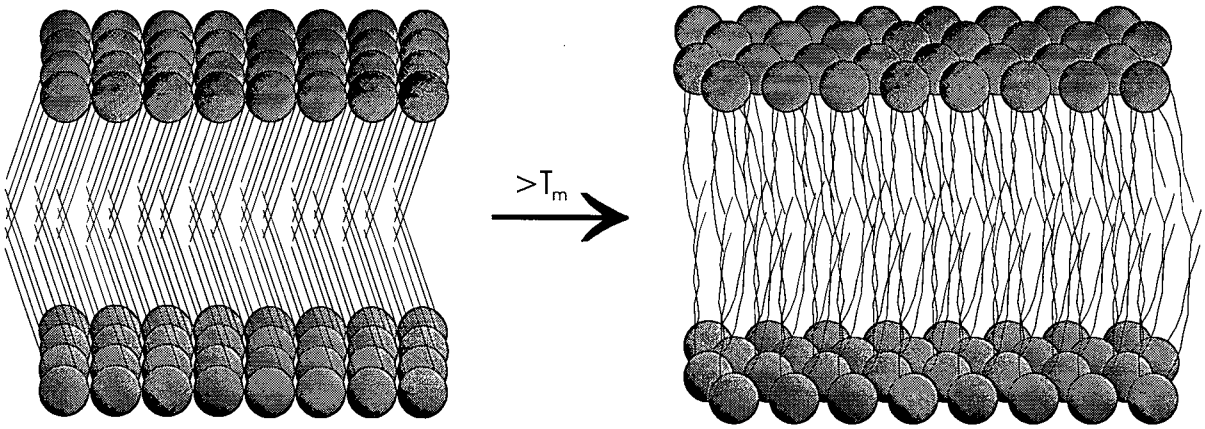

Figure 4. Schematic representation of lipid bilayers during phase transition

The T_m of various lipid bilayers is determined by a number of factors. The headgroup, fatty acyl chain, pressure, temperature, ionic strength, and pH all play a role in determining the T_m (Gennis, 1989). Headgroups, which interact extensively with one another, increase the energy required to distant the lipid molecules in the lipid crystalline state, thus raising the T_m. An increase in pressure elevates the T_m by enhancing the stability of the gel state. The pH and the presence of certain divalent cations could also affect the interaction between neighbouring headgroups. With Ca^{2+} ions at appropriate pH, the T_m of anionic bilayer-lipids increases due to a decrease in repulsion between headgroups. In addition, the length and the degree of unsaturation of the fatty acyl chains also have a huge impact on the T_m. In general, for saturated fatty acyl chains, long acyl

chains increase the T_m by increasing van der Waals interaction between lipid molecules. In the case of unsaturated fatty acyl chains, cis-double bonds introduce kinks which disrupt the packing of the lipid bilayer. This disruptive effect reduces the interaction between acyl chains and consequently lowers the T_m.

1.1.4 Effects of cholesterol on lipid bilayer

Cholesterol, the most common sterol found in membranes, is a compact, rigid hydrophobic entity with a polar hydroxyl group (Figure 5). When incorporated into lipid bilayer, this molecule integrates in between adjacent phospholipid molecules. The hydroxyl group of cholesterol is positioned next to the carbonyl ester of lipid headgroups, and the rigid hydrophobic rings are located in the vicinity of the acyl chains. The hydrophobic portion of cholesterol interacts extensively with the hydrocarbon chains, while the polar hydroxyl group does not interact with the lipid headgroups (Gennis, 1989).

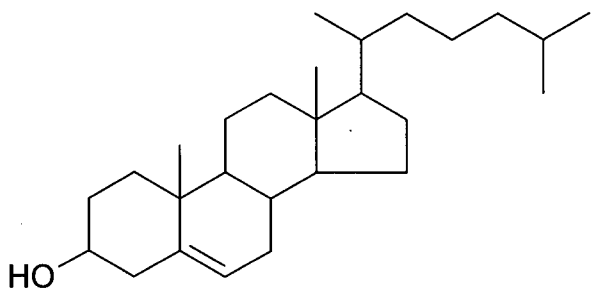

Figure 5. Structure of cholesterol

A unique characteristic of cholesterol is its ability to alter the fluidity of membranes. Cholesterol increases the membrane fluidity at temperatures below T_m, while it decreases the fluidity at temperatures above T_m. The presence of cholesterol in lipid bilayers at 30 mol% or higher can decrease the enthalpy of the phase transition to 0 kcal/mol, hence the sharp phase transition between the gel and liquid crystalline states at T_m is eliminated (Estep et al., 1979). The rationale behind this unique property lies in the rigidity of the cholesterol molecule. In the gel state, the rigid structure of cholesterol disrupts the interaction between acyl chains, thus increasing the fluidity. However, in the liquid-crystalline state, rigid cholesterol molecules constrain the molecular movement of acyl chains. This increases the level of interaction between acyl chains, thus decreasing the fluidity. Therefore at 30 mol% or higher, cholesterol can eliminate phase transition. Through eliminating phase transition, lipid bilayers remain intact over a wide range of temperature. This enhanced integrity allows effective retention of entrapped materials within liposomes.

1.2 Liposomes

1.2.1 Lamellarity of liposomes

Liposomes are lipid vesicles consisting of an internal compartment. Hydration of bilayer-forming lipids leads to the spontaneous formation of multilamellar vesicles (MLVs) (Figure 6A). MLVs consist of multiple lipid vesicles, resembling "vesicles within vesicles" or "concentric onion rings". With a lipid-filled interior, MLVs possess a low entrapped volume (~ 0.5 μL/μmol lipid) despite their huge external diameter (up to 10 μm). To increase the entrapped volume, various techniques have been used to make unilamellar vesicles. Techniques such as sonication, injection of ethanolic solution of lipids into aqueous phase, and French Press shearing can create small unilamellar vesicles (SUVs; Figure 6C) with a diameter of less than 50 nm (Huang, 1969; Barenholz et al., 1979; Gennis 1989). Although these techniques produce unilamellar lipid vesicles with uniform and controllable sizes, SUVs possess a very small entrapped volume (0.5 to 1.0 μL/μmol lipid) because of their small diameter (Stamp and Juliano, 1979; Szoka and Papahadjopoulos, 1980). In addition, the small diameter also leads to a high degree of surface curvature which makes SUVs prone to fusion. This intrinsic instability has led to the use of unilamellar vesicles with a greater diameter. Several methods have been used to make large unilamellar vesicles (LUVs) with diameters ranging from 50 to 500 nm (Figure 6B), including detergent dialysis, infusion and reverse phase evaporation, and fusion methods (Gennis, 1989). In 1985, Hope et al. have devised high pressure extrusion techniques to make LUVs. By extruding through polycarbonate filters with known pore

sizes, LUVs with defined diameter can be produced. This method is very convenient and gives more reproducible liposome size than other techniques. The advantages of LUVs are their resistance to fusion and large entrapped volumes, with 1.5 μL/μmol lipid for 100 nm vesicles. Therefore, LUVs are unilamellar membrane models optimal for encapsulating a wide range of chemicals.

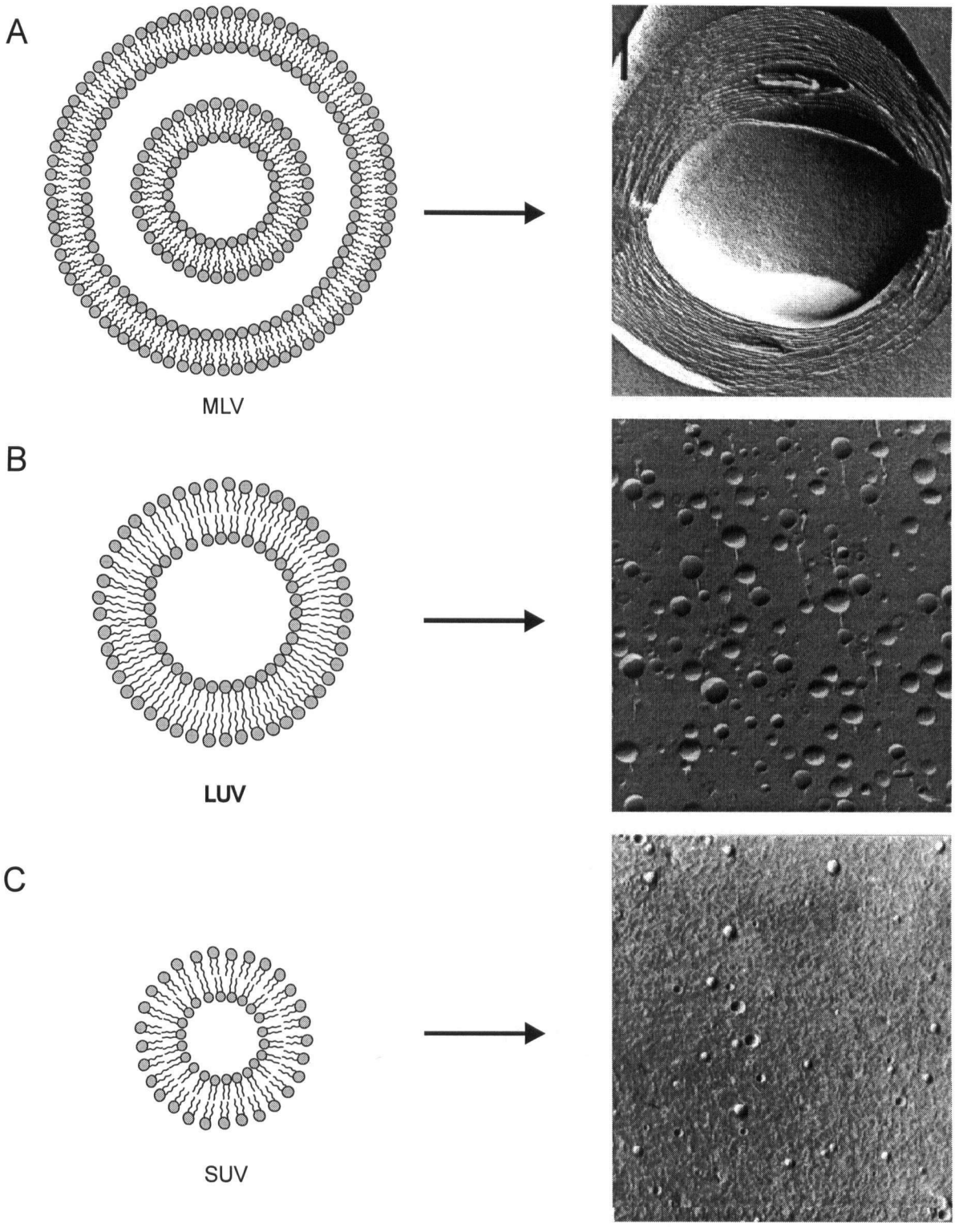

Figure 6. Schematic representation and freeze-fracture micrographs of MLV, LUV and SUV. The bar (black) in micrograph A represents 200 nm in length.

1.2.2 Liposomes as drug carriers

The selective permeability of lipid bilayers gives liposomes the ability to retain charged and polar entities within their internal aqueous compartment. Being enclosed by lipids, entrapped chemicals are isolated from the external environment, thus minimizing any undesirable interactions with extraliposomal materials. This ability to isolate encapsulated chemicals, together with the biological compatibility of natural lipids, make liposomes excellent carriers for intravenous administration of many chemical reagents.

Due to the toxic side effects of many antitumour reagents, intravenous administration of these drugs in their free forms was performed at low levels. But after encapsulation methodologies were available, higher doses can be administered because of the reduced toxic side effects achieved through encapsulation within LUVs. Encapsulated doxorubicin inside LUVs has shown superior therapeutic activity against tumours over their free forms (Mayer et al., 1990; Masood et al., 1993). Hence, LUVs can be employed to deliver high levels of encapsulated drugs while minimizing undesirable side effects.

1.2.3 Passive and active targeting of liposomes

Targeting is a characteristic which delivers materials to specific tissues. Liposomes have been shown to be able to preferentially accumulate at tumour tissues through passive and active targeting.

(i) Passive targeting:

100 nm LUVs are relatively large entities in serum. In circulation, these LUVs are too large to penetrate into healthy tissues. However, the vasculature at tumour tissues is not perfectly formed, thus 100 nm LUVs can penetrate through blood vessels and accumulate in tumours (Bally et al., 1990). This characteristic of 100 nm liposomes is known as passive targeting. Therefore, passive targeting increases the anti-tumour efficacy of encapsulated drugs in comparison to their free form.

(ii) Active targeting:

Advancement in coupling techniques makes the coupling of various ligands onto liposomes possible. With the appropriate ligands on their surface, liposomes can be actively targeted to specific tissues expressing certain receptors. As a result, ligand-conjugated lipid vesicles would preferentially accumulate at tissues expressing the corresponding ligand receptors. Lee and Low (1995) have demonstrated the accumulation of folate-conjugated liposomes in cells overexpressing folate receptors.

With the ability to actively and passively target to specific tissues, the anti-tumour therapeutic activity of encapsulated drugs increases. Therefore, the use of liposomes as a drug carrier is very beneficial for intravenous applications.

1.3 Doxorubicin

1.3.1 Characteristics of doxorubicin

Doxorubicin is a potent antineoplastic agent isolated from *Streptomyces peuceticus*. As shown in Figure 7, doxorubicin is an amphipathic molecule with a hydrophilic amino sugar moiety and a hydrophobic anthraquinone portion. Because of the various functional groups on this antibiotic, doxorubicin can be charged or neutral depending on the pH of the environment. The pK_a of the sugar amine is 8.15, while the pK_a of the phenolic hydroxyl group is 10.1 (Bouma et al., 1986). Hence at pH between 8.15 and 10.1, doxorubicin is neutral. The neutral form of doxorubicin can complex with various metal ions. As reported by Bouma et al. (1986), neutral doxorubicin forms complexes with Fe^{3+} (18.0), Cu^{2+} (12.7), Th^{4+} (10.3), Tb^{3+} (7.2), Pb^{2+} (7.0), Mn^{2+} (7.0), Fe^{2+} (6.5), Zn^{2+} (4.5), Mg^{2+} (3.7) and Ca^{2+} (3.3) with relatively high affinity (the pK_D of these doxorubicin-metal complexes are shown in parentheses).

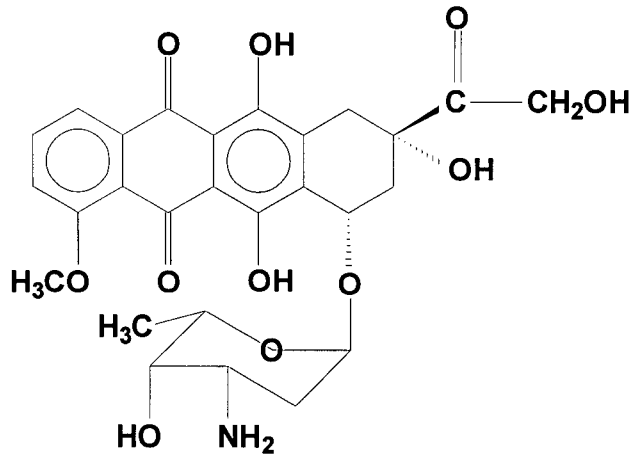

Figure 7. Structure of doxorubicin

Doxorubicin can bind to DNA, lipid, and proteins (de Wolf et al., 1993). The ability of doxorubicin to interact strongly with these biological molecules can inhibit DNA replication, RNA transcription, signal transduction, and protein activity, thus making doxorubicin an effective agent against a wide variety of human tumours. However, intravenous administration of doxorubicin is associated with severe toxic side effects such as cumulative dose-limiting cardiotoxicity and myelosuppression (Blum and Carter, 1974; Benjamin, 1975; Herman et al., 1983; Rahman et al., 1986; Bally et al., 1990). Therefore, the encapsulated form of doxorubicin has been employed for intravenous administrations in order to reduce the undesirable side effects.

1.3.2 Encapsulation of doxorubicin

The amphipathic nature of doxorubicin makes it an excellent candidate to be encapsulated. Various encapsulation methods rely on the sugar amine of doxorubicin; because when protonated, its positive charge enables doxorubicin to be retained in the internal aqueous compartment of liposomes. Once encapsulated inside liposomes composed of strong bilayer forming lipids, doxorubicin is also retained very efficiently inside liposomes (Lasic et al., 1995). Therefore, doxorubicin is a suitable agent to be encapsulated.

Both passive and active encapsulation methods have been devised for doxorubicin. Passive encapsulation methods, such as the hydration of dried lipid film with doxorubicin solution (Rahman et al., 1986; Amselem et al., 1990) and the incorporation of negatively charged lipids into the liposomal composition (Crommelin and von Bloois, 1983) have been used initially. However, these passive entrapment methods can only achieve low levels of drug encapsulation. Improvement in the encapsulation efficiency can be achieved using active encapsulation methods. Since only the neutral form of doxorubicin can pass readily through the lipid bilayer, doxorubicin has been loaded with a transmembrane proton gradient (Mayer et al., 1986, 1993; Haran et al., 1993; Harrigan et al., 1993). Upon encountering the intraliposomal pool of protons, neutral doxorubicin becomes protonated. The protonated form of doxorubicin is positively charged and is impermeable through the lipid bilayer, thus it remains inside the liposomes. In addition, doxorubicin has been reported to form a gel with SO_4^{2-} or

precipitate inside liposomes, hence this characteristic further enhances the retention property of doxorubicin (Haran et al., 1993; Lasic et al., 1995).

Two of the methods to actively load doxorubicin through a transmembrane proton gradient include the low pH citrate and the ammonium sulfate methods. The mechanisms behind these methods are shown in Figure 8 and 9. In Mayer's low pH citrate method (Figure 8), unprotonated neutral doxorubicin in the pH 7.4 extraliposomal media can pass through the lipid bilayer and penetrate into the liposomal interior. Once inside the liposomes, doxorubicin becomes protonated in the low pH environment and thus is retained inside the liposomes. A citrate buffer at pH 4.0 is used as the source of protons because of its strong buffering capacity. At this pH, the three carboxylic acid groups of citrate, with pK_a values of 3.06, 4.74 and 5.40, enable one citrate molecule to protonate up to two doxorubicin molecules inside the liposomes.

In Haran's ammonium sulfate method (Figure 9), neutral ammonia can go to the outside by dissociating a proton from the entrapped positively charged ammonium ion, thus building up a transmembrane proton gradient. Neutral doxorubicin from the extraliposomal media can be protonated in the intraliposomal space upon encountering the pool of protons. One molecule of ammonium sulfate (i.e. two molecules of NH_4^+) can lead to the protonation of two doxorubicin molecules within liposomes. Both the low pH citrate and the ammonium sulfate methods could encapsulate high level of doxorubicin close to 100 % efficiency.

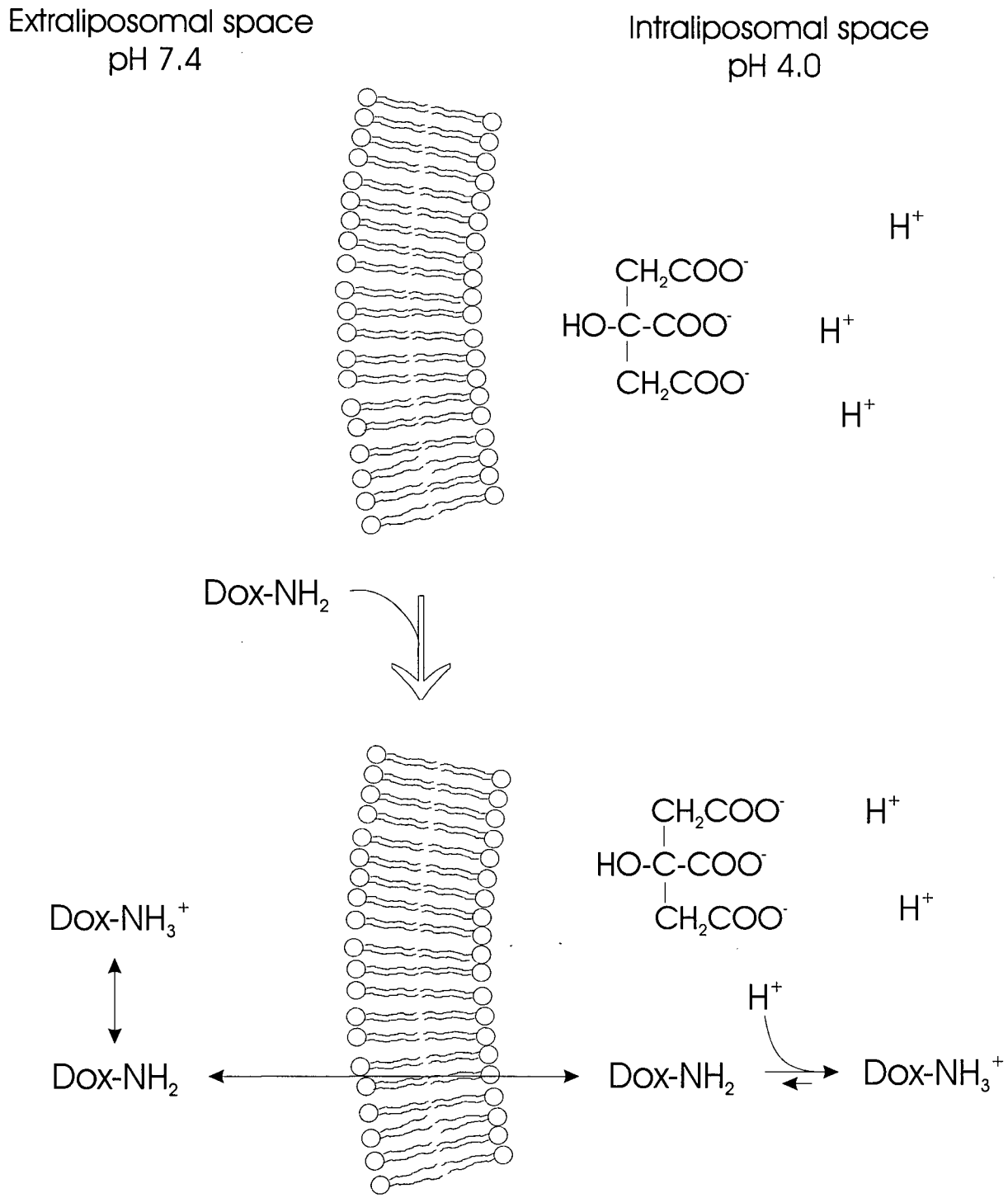

Figure 8. Loading of doxorubicin into liposomes with a transmembrane pH gradient

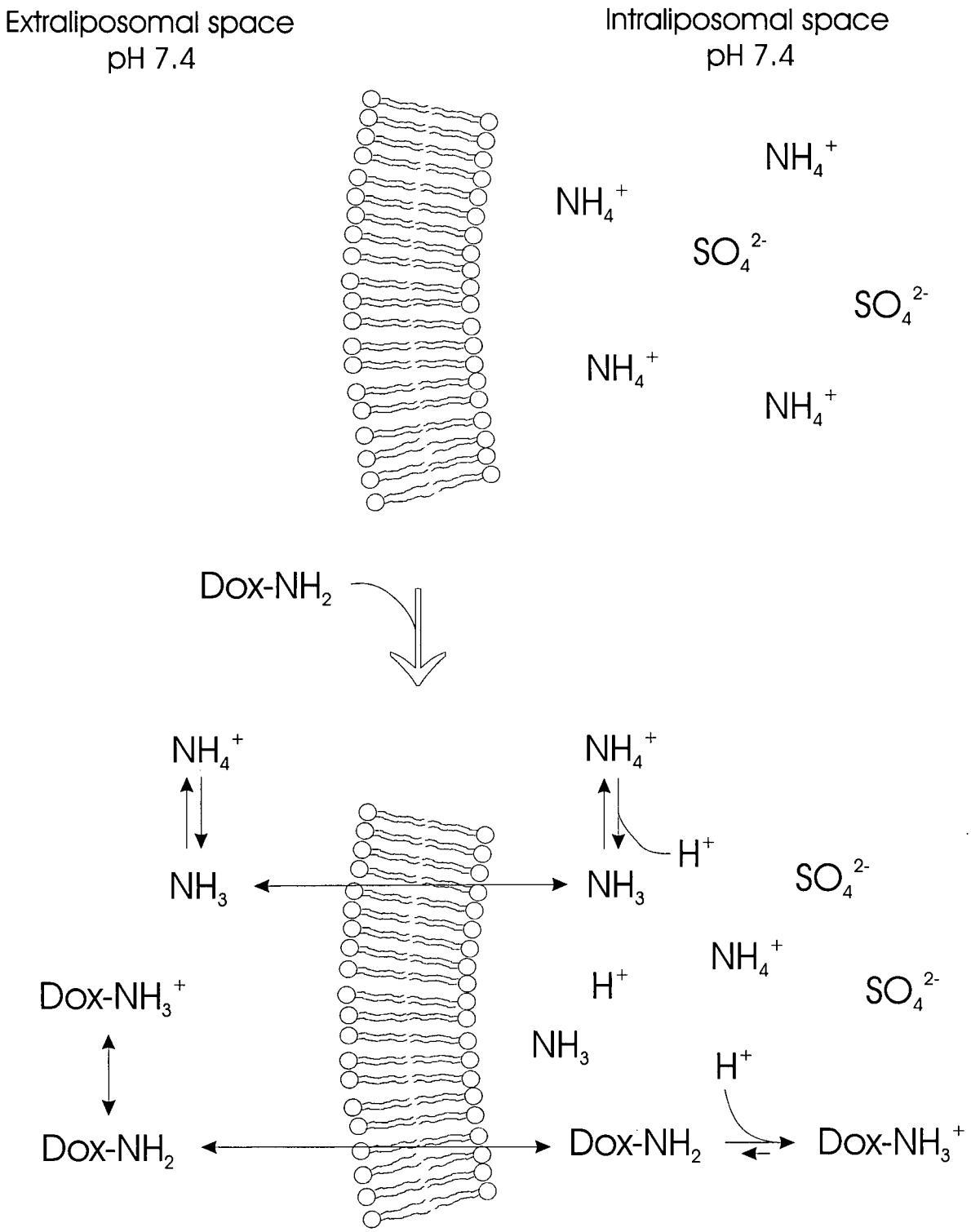

Figure 9. Loading of doxorubicin into liposomes with a transmembrane ammonium sulfate gradient

Recently, weakly basic drugs such as vincristine and ciprofloxacin have been shown to be actively encapsulated into $MnSO_4$-containing liposomes in the presence of the ionophore A23187 (Fenske et al., 1998). The structure of A23187 is shown in Figure 10. This calcium ionophore in its dimeric form is capable of translocating divalent cations such as Ni^{2+}, Co^{2+}, Zn^{2+}, Mn^{2+}, Mg^{2+}, Ca^{2+}, Sr^{2+}, and Ba^{2+} across the lipid bilayer in exchange for two protons (Chapman et al., 1987).

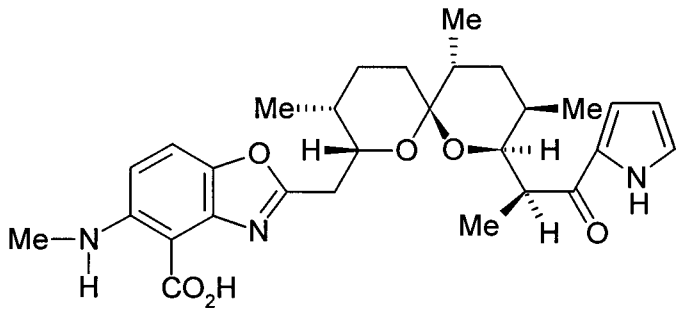

Figure 10. Structure of ionophore A23187

The role of A23187 in this method is to establish an acidic liposomal interior by exchanging one Mn^{2+} ion for the inward movement of two protons. Therefore, each entrapped Mn^{2+} ion results in the exchange of two protons to the internal compartment, which consequently leads to the encapsulation of two drug molecules. This method has been studied in this thesis and found to also load doxorubicin efficiently. The mechanism of the A23187 method in loading doxorubicin is illustrated in Figure 11.

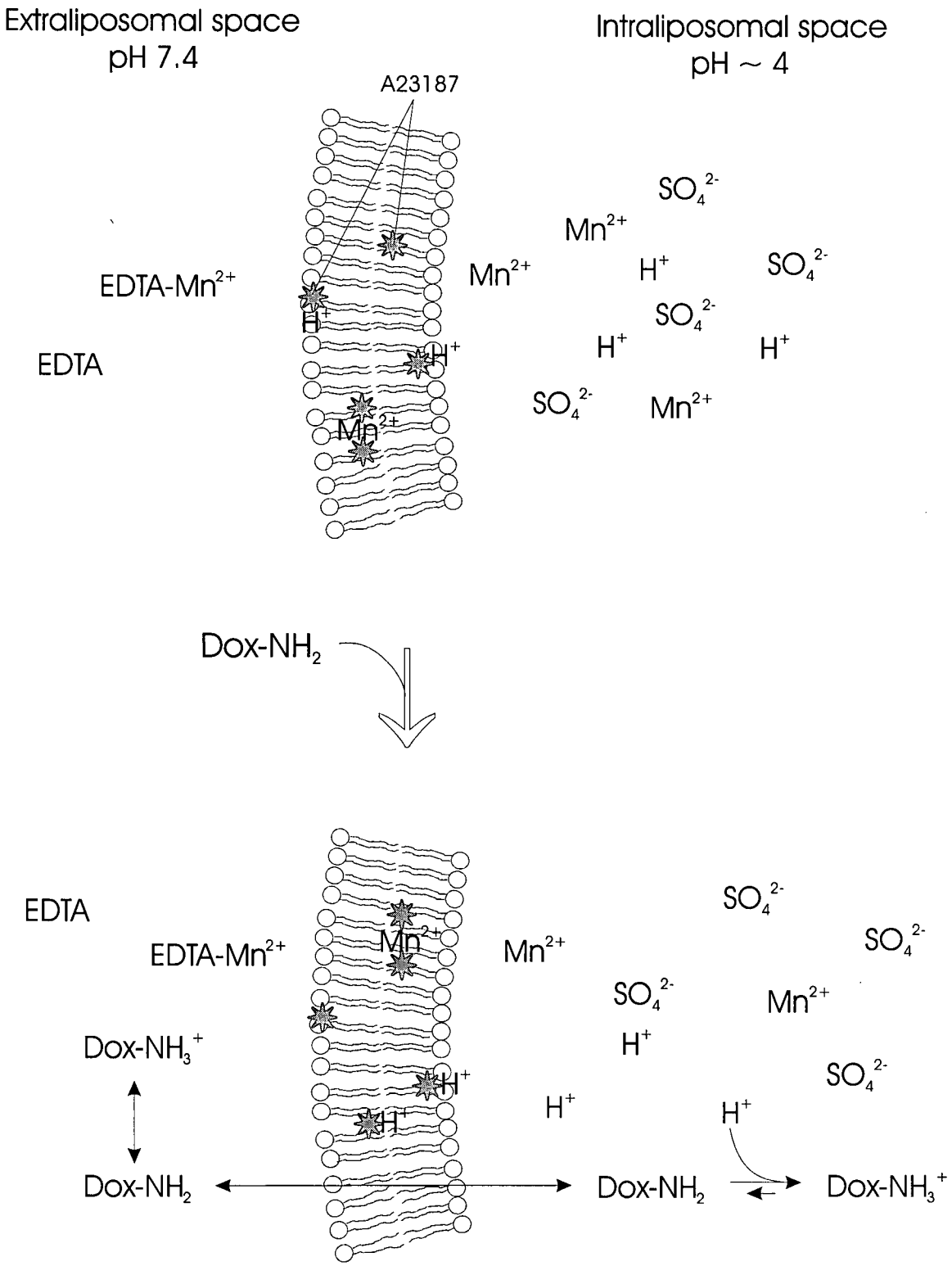

Figure 11. Loading of doxorubicin using the A23187 ionophore method

1.4 Use of 100 nm-Egg Sphingomyelin/Cholesterol (55/45 mol%) liposomes for drug encapsulation

Egg Sphingomyelin:

Sphingomyelin is a natural phospholipid present in many animal cell and bacterial membranes (Gennis, 1989). In combination with cholesterol, sphingomyelin can form rigid bilayer structure due to strong van der Waals interactions between the lipid acyl chains and cholesterol (McIntosh et al., 1992). The tight interaction between sphingomyelin and cholesterol results in superior retention properties of egg sphingomyelin/cholesterol (55/45 mol%) liposomes over DSPC/cholesterol (55/45 mol%) lipid vesicles for the antitumour drug vincristine (Webb, 1995).

Cholesterol:

Besides eliminating the phase transition at 30 mol% or higher (see 1.1.4), the incorporation of cholesterol into liposomes also increases the circulation lifetime of lipid vesicles (Patel et al., 1983; Semple et al., 1996). Cholesterol reduces the disruptive effects of plasma proteins on the lipid bilayer, thus enhancing the integrity of liposomes. Cholesterol has also been reported to impart bilayer rigidity (Kulkarni et al., 1995). The enhanced rigidity and stability induced by the presence of cholesterol are additional reasons for the inclusion of cholesterol in liposomes used for drug encapsulation.

100 nm in diameter:

100 nm-liposomes have been shown to exhibit extended circulation half-life and they are very effective against tumours (Mayer et al., 1989). Therefore, for optimal drug retention, 100 nm-liposomes composed of egg sphingomyelin/cholesterol at 55/45 mol ratio are the choice for encapsulating doxorubicin.

1.5 Thesis objective

The enhanced drug cytotoxicity reported for various doxorubicin-metal complexes (Gutteridge, 1984; Muindi et al., 1984; Hasinoff, 1989; Greenaway and Dabrowiak, 1982; Hasinoff et al., 1989) has led to the development of a liposomal doxorubicin loading technique that relies on the formation of drug-metal ions complexes. The high affinity between doxorubicin and various metal ions provides the driving force necessary for the active drug loading process. Among all these metal ions, Mn^{2+} is chosen in this study because of two reasons: Mn^{2+} can form complex with doxorubicin and can also be used to load doxorubicin in the presence of the ionophore A23187. Therefore $MnSO_4$-containing liposomes are used to load doxorubicin in order to compare the drug loading effectiveness of the complex formation method with the pH gradient method using the A23187 ionophore.

Chapter 2
Encapsulation of doxorubicin by forming drug-metal complexes

2.1 Introduction

Doxorubicin is a potent antineoplastic agent active against a wide range of human cancers. However, treatment with doxorubicin is associated with severe toxic side effects which include cumulative dose-limiting cardiotoxicity and myelosuppression (Blum and Carter, 1974; Benjamin, 1975; Herman et al., 1983; Rahman et al., 1986; Bally et al., 1990). When administered by intravenous (i.v.) injection, the use of liposomes to encapsulate doxorubicin can reduce toxic side effects without decreasing drug potency (Rahman et al., 1980, 1986; Herman et al., 1983; Gabizon et al., 1985; Mayer et al., 1989; Szoka, 1991; Vaage et al., 1997; Daemen et al., 1997).

Doxorubicin is an amphipathic weak base consisting of an anthraquinone moiety (the aglycone part) and an amino sugar. Previous work has shown that doxorubicin and other weak bases can be accumulated into vesicles with an acidic interior as a consequence of the transmembrane pH gradient (Mayer et al., 1986, 1993; Harrigan et al., 1993). Recently, a new method for drug loading has been developed using LUVs containing Mn^{2+} in the presence of the ionophore A23187 (Fenske et al., 1998). The ionophore A23187 translocates one Mn^{2+} ion to the outside of the LUV in exchange for the inward movement of two protons, thereby generating a pH gradient (interior acidic) across the bilayer which consequently drives drug uptake. Efficient loading of

vincristine and ciprofloxacin has been demonstrated using this method (Fenske et al., 1998). In this thesis, Fenske's ionophore method was used to also load doxorubicin. However, it was found that doxorubicin can be efficiently loaded into liposomes with a transmembrane Mn^{2+} gradient in the absence of ionophore via the formation of intravesicular doxorubicin-Mn^{2+} complexes. It is shown that complex formation between doxorubicin and Mn^{2+} provides a strong driving force for doxorubicin accumulation inside liposomes.

2.2 Materials and Methods

Materials:

Egg sphingomyelin was purchased from Northern Lipids Inc. (Vancouver, BC). Cholesterol and the calcium ionophore A23187 were obtained from Sigma Chemical Co. (Mississauga, ON). Doxorubicin hydrochloride (Adriamycin) was manufactured by Pharmacia & Upjohn (Don Mills, ON). ^{14}C-Mevalonic acid (RS-[2-^{14}C]Mevalonic acid, DBED salt) was purchased from Amersham Canada Limited (Oakville, ON). ^{3}H-Cholesteryl hexadecyl ether (^{3}H-CHE) was produced by NEN Life Science Products (Boston, MA). ^{14}C-Methylamine (^{14}C-methylamine hydrochloride) was purchased from DuPont (Boston, MA). Sterile mouse serum was obtained from Cedarlane Laboratories Limited (Hornby, ON). Nuclepore polycarbonate filters (25 mm 0.1 μm pore size) were obtained from Costar Scientific Corporation (Toronto, ON). All chemicals were reagent grade.

Methods:

Preparation of 100 nm large unilamellar vesicles (LUVs): Liposomes were prepared by the freeze-thaw extrusion method as described previously by Hope et al. (1985). Throughout this study, 100 nm diameter large unilamellar vesicles consisting of sphingomyelin/cholesterol (55/45 molar ratio) were used, because they have been shown to exhibit excellent retention properties (Webb et al., 1995). Briefly, mixtures of sphingomyelin and cholesterol (55/45 mole ratio) were dissolved in 2-methylpropan-2-ol at 60 °C. A trace amount of ^{3}H-CHE was added to achieve a final activity of 0.05 μCi/μmol lipid, and the solution was then frozen in liquid nitrogen. This frozen material was lyophilized for at least 4 h under high vacuum to remove the organic solvent. Unless specified otherwise, the lyophilized lipid mixture was then hydrated at 50 mM with a buffer containing 0.30 M $MnSO_4$ and 30 mM Hepes (pH 7.4) in a 60 °C water bath. This suspension was subjected to five freeze-thaw cycles by alternating between liquid nitrogen and a 60 °C water bath with vigorous vortexing between cycles. Subsequently, the hydrated lipid mixture was extruded 10 times through two layers of polycarbonate filters with pore size of 0.1 μm at 60 °C using a water-jacketed extruder (Lipex Biomembranes Inc., Vancouver). Phospholipid content of the LUVs was measured employing Fiske-Subbarow phosphate assay (Fiske and Subbarow, 1925). The phospholipid content, together with the ^{3}H dpm from ^{3}H-CHE lipid marker, was used to determine the specific activity of the liposomes (expressed as dpm/nmol total lipid including cholesterol). The specific activity of liposomes was used for quantification of the lipid concentration.

Doxorubicin uptake experiments: A transmembrane Mn^{2+} gradient was generated across the LUVs by exchanging the extraliposomal buffer using Sephadex G-50 spin columns (Harrigan et al., 1993). Subsequently, the lipid concentration was determined by liquid scintillation counting. Unless specified otherwise, all experiments involving the ionophore A23187 used buffer containing 0.30 M sucrose, 20 mM Hepes and 15 mM EDTA at pH 7.4; experiments performed in the absence of the ionophore employed buffer containing 0.30 M sucrose and 20 mM Hepes at pH 7.4. The transition temperatures of sphingomyelins range from 40.5 to 57 °C (Marsh, 1990); as a consequence, all uptake experiments were performed at 60 °C in order to permit efficient partitioning of the drug into and across the lipid bilayer. When present, A23187 was used at a concentration of 0.1 μg ionophore/μmol lipid and LUVs were incubated with the ionophore at 60 °C for 5 min prior to the addition of doxorubicin. The amount of doxorubicin used in each experiment varied depending on the desired drug-to-lipid molar ratio. After the addition of doxorubicin, the lipid concentration was 5 mM. Samples of this mixture were taken at specific time points, applied onto spin columns and centrifuged at 760 x g for 2 min. This step removes the unencapsulated doxorubicin, leaving liposomes with encapsulated doxorubicin in the eluant. In order to determine the drug-to-lipid molar ratio, part of the eluant was subjected to liquid scintillation counting to assay for the amount of lipid, while another part was added to a solution of 1.0 % Triton X-100, 2.0 mM EDTA and 20 mM Hepes (pH 7.5) for the quantification of doxorubicin by absorption spectroscopy at 480 nm ($\varepsilon = 1.06 \times 10^4\ M^{-1}\ cm^{-1}$ (De Wolf et al., 1993)). The total drug-to-lipid molar ratio (100 % value) in the uptake mix was

determined at specific time points by the same procedure but omitting the spin column centrifugation step.

Determination of pH gradients: To determine the pH gradient (inside acidic) present across the lipid bilayer, a trace amount of ^{14}C-methylamine (Rottenberg, 1979) was added to the uptake cocktail (final activity = 0.2 μCi/mL). The doxorubicin uptake experiments were performed as described above, except dual ^{3}H- and ^{14}C-radioisotope liquid scintillation counting was used. Assuming a trapped volume of 1.5 μL per μmol lipid for 100 nm diameter LUVs (Hope et al., 1985; Veiro and Cullis, 1990), intraliposomal and extraliposomal methylamine concentrations could be determined. The pH gradient (ΔpH) can then be calculated by (Rottenberg, 1979; Harrigan et al., 1992):

$$\Delta pH = \log \{[H^+]_{inside}/[H^+]_{outside}\} = \log \{[methylamine]_{inside}/[methylamine]_{outside}\}$$

For the determination of ΔpH in LUVs with a basic interior, ^{14}C-mevalonic acid was used instead of ^{14}C-methylamine (Harrigan et al., 1992).

Absorption spectra: The effect of Mn^{2+} on the doxorubicin absorption spectrum was determined by mixing various concentrations of $MnSO_4$ with doxorubicin (54 μM final concentration) in 100 mM Hepes (pH 7.4). Absorption spectra from 350 to 700 nm were taken using a Shimadzu UV160U Spectrophotometer. Then, at saturating concentration of Mn^{2+}, the pH dependence of the doxorubicin-Mn^{2+} complex was also

studied. 400 mM $MnSO_4$, 24 μM doxorubicin and 100 mM of various buffers were used: MES as the buffer for pH 5.2 and 5.6, Pipes buffer for pH 6.0, 6.4 and 6.8 and Hepes was used at pH 7.2, 7.5, 7.8 and 8.0. Spectra of doxorubicin loaded in the presence or absence of A23187 were compared with the spectrum of unencapsulated doxorubicin in the presence of empty liposomes.

***In vitro* leakage assay**: Doxorubicin was loaded at a drug-to-lipid ratio molar of 0.5 (mol/mol) in the presence or absence of A23187. Each uptake mixture was incubated for 70 min at 60 °C after which it was applied onto spin columns to remove unencapsulated doxorubicin. After centrifugation, an equal volume of sterile mouse serum was added followed by incubation at 37 °C for up to 24 h. The final concentration of liposomes was 1 mM. Aliquots were taken out at specified time points for the determination of doxorubicin retention.

2.3 Results

2.3.1 Remote loading of doxorubicin into $MnSO_4$-containing liposomes using the ionophore A23187

Previous studies (Fenske et al., 1998) have shown that amino-containing drugs such as vincristine and ciprofloxacin can be loaded into liposomes exhibiting a Mn^{2+} gradient in the presence of ionophore A23187 and external EDTA. In this thesis, this method has been characterized and found to load doxorubicin efficiently. The kinetics of doxorubicin loading into 100 nm diameter LUVs at 60 °C is shown in Figure 12A. The transbilayer pH gradient was also measured, demonstrating an initial pH gradient of 3.4 units (inside acidic). Upon drug addition, this gradient was quenched within 5 min. However, the ΔpH was later re-established, rising to 2.4 units at t = 90 min. The magnitude of the re-established ΔpH varied depending on the drug-to-lipid molar ratio used in the experiment (Figure 12B).

The disappearance and subsequent recovery of the acidic gradient was accompanied by marked colour changes: the solution was initially red in colour (t = 0) and then turned purple within 5 min. After 45 min, the colour changed back to red. The transient purple colour could not be due to the change of the internal pH, since doxorubicin turns purple only at pH values higher than 8 (results not shown). The ^{14}C-mevalonic acid data show that no basic pH gradient was generated throughout the entire uptake process (Figure 12A). This means that the highest intraliposomal pH at any point during drug uptake was equivalent to the extraliposomal pH (i.e. pH 7.4).

Figure 12 (A): Time course of doxorubicin uptake using A23187 (●) into LUVs containing $MnSO_4$ (0.30 M). The acidic (❍) or basic (❑) nature of the LUV interior was determined during the uptake process using ^{14}C-methylamine and ^{14}C-mevalonic acid as ΔpH probes, respectively. The colour of the uptake mixture was indicated on top of the diagram. Uptake was performed at a drug-to-lipid molar ratio of 0.53. (B): Final pH gradient (interior acidic) re-established after loading at various drug-to-lipid molar ratios in the presence of A23187. Final pH gradients were determined using ^{14}C-methylamine after an equilibrium interior pH had been established. (C): Time course of doxorubicin uptake in the absence of A23187 (■). The pH of the LUV interior was monitored using ^{14}C-methylamine (❍) and ^{14}C-mevalonic acid (❑) respectively. The colour of the uptake mixture was indicated on top of the diagram. Uptake was performed at a drug-to-lipid molar ratio of 0.45 with an A23187 concentration of 0.1 μg/μmol lipid.

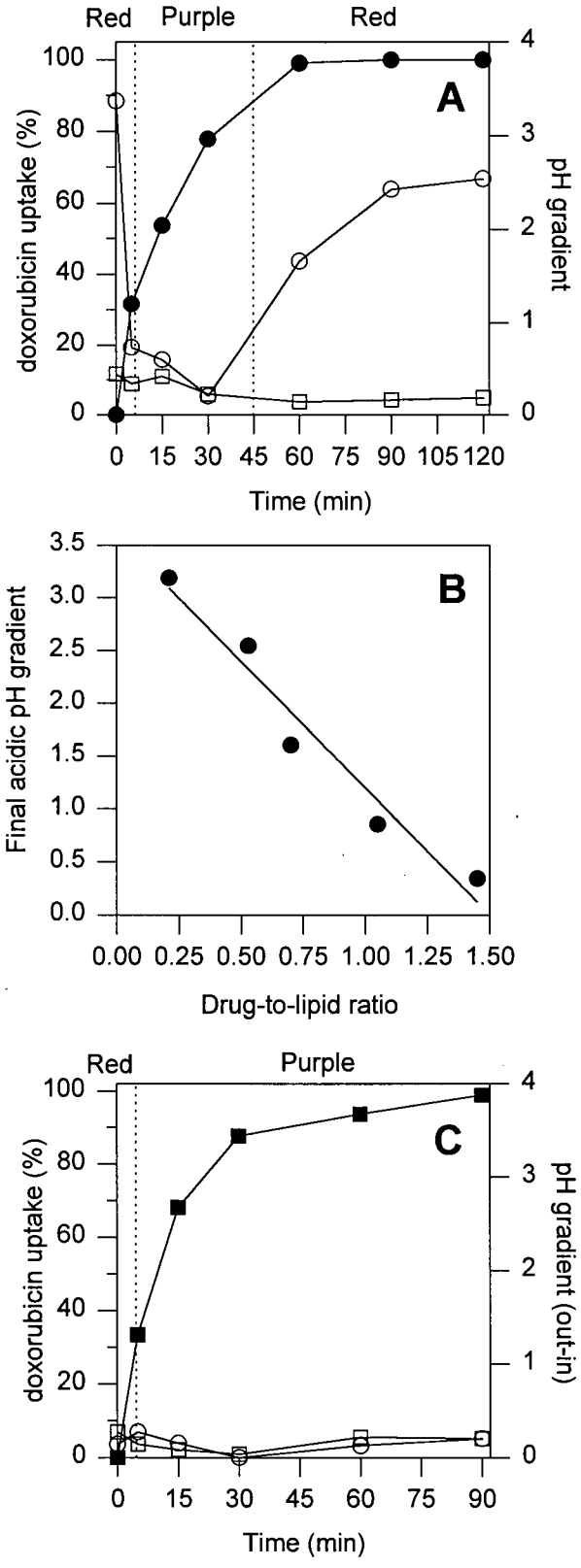
Red
Purple
Red
A
doxorubicin uptake (%)
pH gradient
Time (min)
B
Final acidic pH gradient
Drug-to-lipid ratio
Red
Purple
C
doxorubicin uptake (%)
pH gradient (out-in)
Time (min)

Figure 12

2.3.2 Encapsulation by forming drug-metal complexes

Interestingly, doxorubicin uptake as shown in Figure 12A continued between 5 to 30 min despite the absence of any acidic gradient. This suggested that the pH gradient was not required for doxorubicin uptake. To test this hypothesis, uptake of doxorubicin was examined in the absence of the ionophore A23187. The kinetics of doxorubicin uptake in the absence of A23187 (Figure 12C) are very similar to those in the presence of A23187 (Figure 12A). Only background levels of methylamine or mevalonic acid were found entrapped inside liposomes during uptake in the absence of A23187, indicating that no pH gradient was generated during the uptake process. The intraliposomal and the extraliposomal pH values were stable at pH = 7.4 throughout the uptake process. The solution turned from red to purple within 5 min after uptake had begun, and it stayed purple thereafter.

Doxorubicin was loaded at various drug-to-lipid molar ratios in the presence or absence of A23187, and the loading efficiencies are shown in Figure 13. Both systems demonstrated similar doxorubicin loading efficiencies. Nearly 100 % drug uptake could be achieved up to a drug-to-lipid molar ratio of approximately 0.5. At higher drug-to-lipid molar ratios, the efficiency of drug uptake decreased. Therefore, in order to detect possible differences in uptake levels between different systems, a drug-to-lipid molar ratio of approximately one was used in subsequent experiments which require distinctions between loading efficiency.

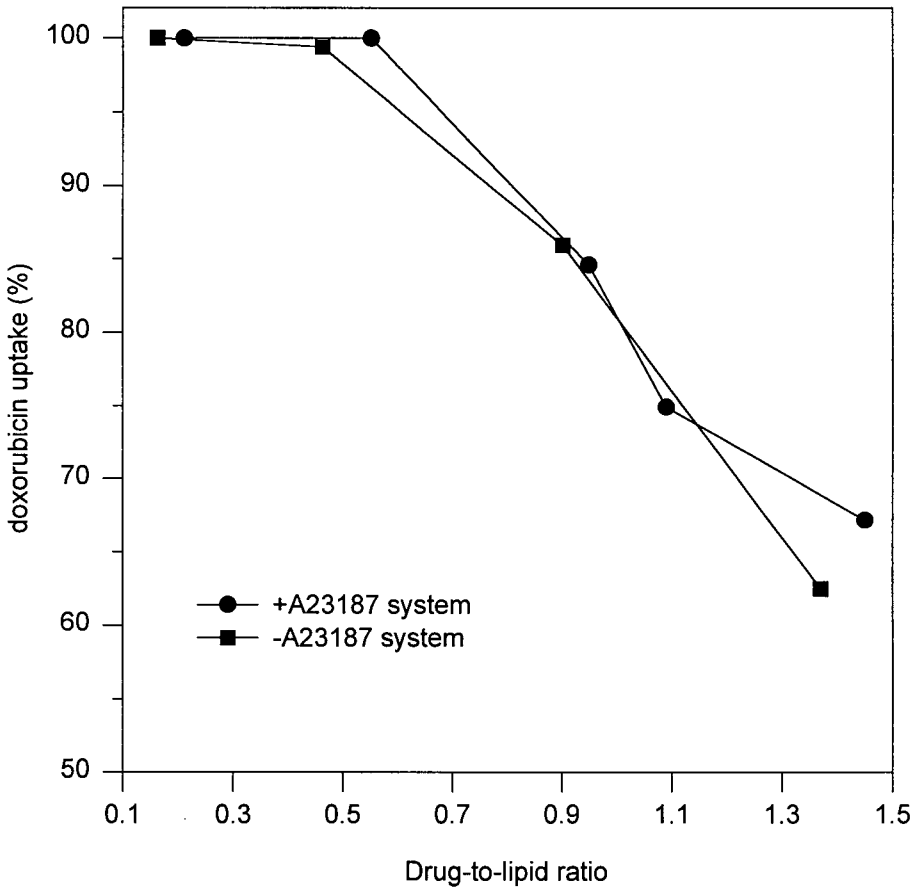

Figure 13. Equilibrium levels of doxorubicin uptake into LUVs containing $MnSO_4$ in the presence (●) or absence (■) of A23187 at various drug-to-lipid molar ratios. All uptake experiments were performed at 60 °C and were continued until the uptake levels became constant (60 to 120 min). LUVs used for both systems were composed of Egg Sphingomyelin/Cholesterol (55:45) and contained 0.30 M $MnSO_4$ titrated to pH 7.4 by 30 mM Hepes.

2.3.3 Complex formation between doxorubicin and Mn^{2+} ions

In order to explore the mechanism of doxorubicin uptake into liposomes exhibiting a transmembrane Mn^{2+} gradient but no pH gradient, the possible formation of doxorubicin-Mn^{2+} complexes was investigated using absorption spectroscopy. Absorption spectra of doxorubicin at pH 7.4 in the presence of various concentrations of $MnSO_4$ are shown in Figure 14A. A gradual red-shift was observed in the spectra upon the addition of Mn^{2+}, and the colour of the solution turned from red to purple at higher Mn^{2+} concentrations. Doxorubicin (54 μM) was found to be saturated with Mn^{2+} at approximately 400 mM $MnSO_4$. Figure 14B shows the change in absorption spectra of the doxorubicin-Mn^{2+} complex (at the saturating concentration of Mn^{2+}) when titrated from pH 5.2 to 8.0. At pH 5.2, most of the complex is dissociated, resulting in an absorption spectrum resembling the characteristic absorption peak for free doxorubicin which has a peak at approximately 480 nm. Between pH 6.0 and 7.8 the spectrum was red-shifted, resulting in a spectrum characteristic of the doxorubicin-Mn^{2+} complex. A further increase in pH beyond 8.0 caused precipitation of Mn^{2+}. The absorbance of the doxorubicin-Mn^{2+} complexes varies significantly over a wide range of wavelengths between pH 5.2 to 8.0, with the most drastic changes at 580 nm. Since complex formation only occurs when the sugar amine is neutral, so the colour change is indicative of the degree of protonation of the sugar amine. When plotting the change in A_{580} versus the pH, the apparent pK_a of the doxorubicin sugar amine at saturating Mn^{2+} concentration was determined to be approximately 6.6 (Figure 14C).

Figure 14. (A): Absorption spectra of doxorubicin in the presence of various concentrations of $MnSO_4$. Doxorubicin (54 μM) was mixed with 0, 2, 10, 50, 100, 200, 400 and 500 mM $MnSO_4$. All solutions were buffered at pH 7.4 by 100 mM Hepes. The colour of the uptake mixture was indicated in parentheses. (B): Absorption spectra of doxorubicin-Mn^{2+} complexes at various pH values. $MnSO_4$ (400 mM) and doxorubicin (24 μM) were buffered using 100 mM concentrations of the following buffers: MES pH 5.2-5.6; Pipes pH 6.0-6.8 and Hepes pH 7.2-8.0. The colour of the uptake mixture was indicated in parentheses. (C): Plot of absorbance (A_{580}) vs. pH. The pK_a of the doxorubicin sugar amine at saturating concentration of Mn^{2+} was determined from the inflection point of the curve (pK_a = 6.6). (D): Absorption spectra of unencapsulated doxorubicin in the presence of empty liposomes (------), and of encapsulated doxorubicin, loaded either in the presence of A23187 (·····) or the absence of A23187 (—·—·). All spectra were obtained at a drug-to-lipid molar ratio of 0.5.

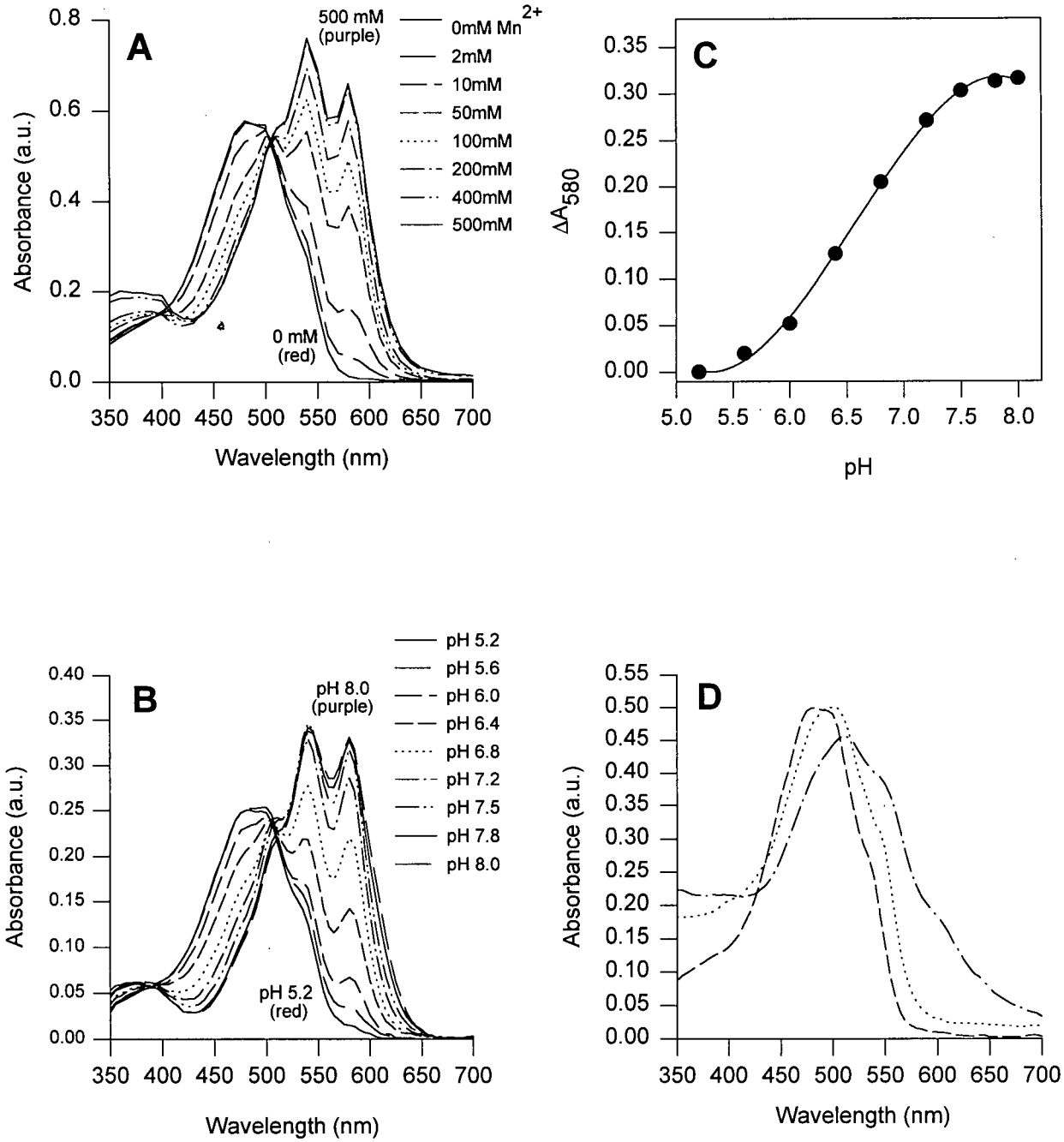
A
500 mM
(purple)
0mM Mn2+
2mM
10mM
50mM
100mM
200mM
400mM
500mM
0 mM
(red)
Absorbance (a.u.)
Wavelength (nm)
C
ΔA580
pH
B
pH 8.0
(purple)
pH 5.2
pH 5.6
pH 6.0
pH 6.4
pH 6.8
pH 7.2
pH 7.5
pH 7.8
pH 8.0
pH 5.2
(red)
Absorbance (a.u.)
Wavelength (nm)
D
Absorbance (a.u.)
Wavelength (nm)

Figure 14

2.3.4 State of doxorubicin inside Mn^{2+}-containing liposomes

The characterization of the liposomal doxorubicin loaded in the presence or absence of A23187 was also performed using absorption spectroscopy. Absorption spectra were taken after doxorubicin had been loaded into liposomes (Figure 14D). As a control, a spectrum of free doxorubicin in the presence of empty liposomes was taken. All spectra were obtained from doxorubicin and liposomes at a drug-to-lipid molar ratio of approximately 0.5. In the absence of A23187, the (loaded) doxorubicin spectrum shifted to higher wavelengths resembling a non-saturating doxorubicin-Mn^{2+} complex spectrum at pH 7.4. In the A23187-containing system, the spectrum of liposomal doxorubicin was identical to that of the unencapsulated doxorubicin, indicating that the doxorubicin was not complexed to Mn^{2+}.

2.3.5 Effects of external pH and entrapped Mn^{2+} levels on complex dependent doxorubicin accumulation

To investigate the influence of the external pH on doxorubicin uptake, the extraliposomal pH (pH_o) in uptake experiments was varied while keeping the intraliposomal pH (pH_i) constant. Figure 15 shows the effect of the pH_o on the loading of doxorubicin into Mn^{2+}-containing liposomes in the absence of A23187 using a drug-to-lipid molar ratio of 1.1. Doxorubicin uptake remained constant from pH 6.0 to 6.5 and gradually increased as the pH_o rose from pH 6.5 to 8.0. By measuring the pH gradients during these uptake processes, it was found that the pH_i became equal to the pH_o as soon as drug uptake had begun (data not shown), regardless as to whether the initial pH gradient across the lipid bilayer was due to an acidic or basic interior.

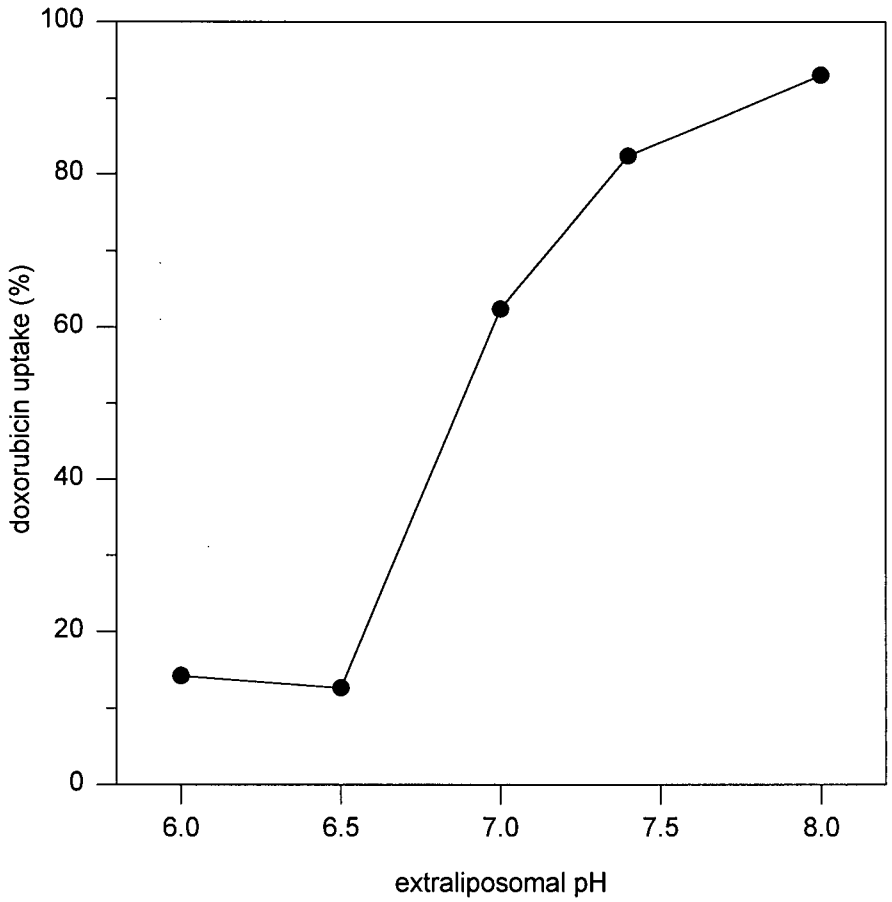

Figure 15. Effect of extraliposomal pH on doxorubicin uptake in the absence of A23187. All uptake experiments employed 0.30 M $MnSO_4$ + 30 mM Hepes (pH 7.4) containing liposomes and doxorubicin was loaded at a drug-to-lipid molar ratio of 1.1. In the extraliposomal buffers, Hepes was used to buffer at pH 7.0, 7.4 and 8.0 while Hepes and Pipes were used to buffer at pH 6.0 and 6.5.

The effect of the intraliposomal Mn^{2+} concentration on the level of doxorubicin uptake was investigated for both in the presence and absence of A23187. Liposomes with no Mn^{2+} (employing 0.30 M Na_2SO_4-containing liposomes), 0.15 M, 0.30 M, 0.45 M and 0.60 M $MnSO_4$ (buffered at pH 7.4 with 30 mM Hepes) were used in the uptake experiments. The results in Figure 16A show that 0.30 M Mn^{2+} was sufficient to achieve a high level of drug uptake at a drug-to-lipid molar ratio of 0.96 in the doxorubicin-Mn^{2+} complex formation system. A sharp increase in drug uptake was observed between 0 M and 0.15 M Mn^{2+}, and a further but moderate increase was found between 0.15 M and 0.30 M. The level of drug uptake then leveled off at 85 % at Mn^{2+} concentrations higher than 0.30 M. At a drug-to-lipid molar ratio of 1.0, doxorubicin uptake in the presence of A23187 showed very similar results (Figure 16B).

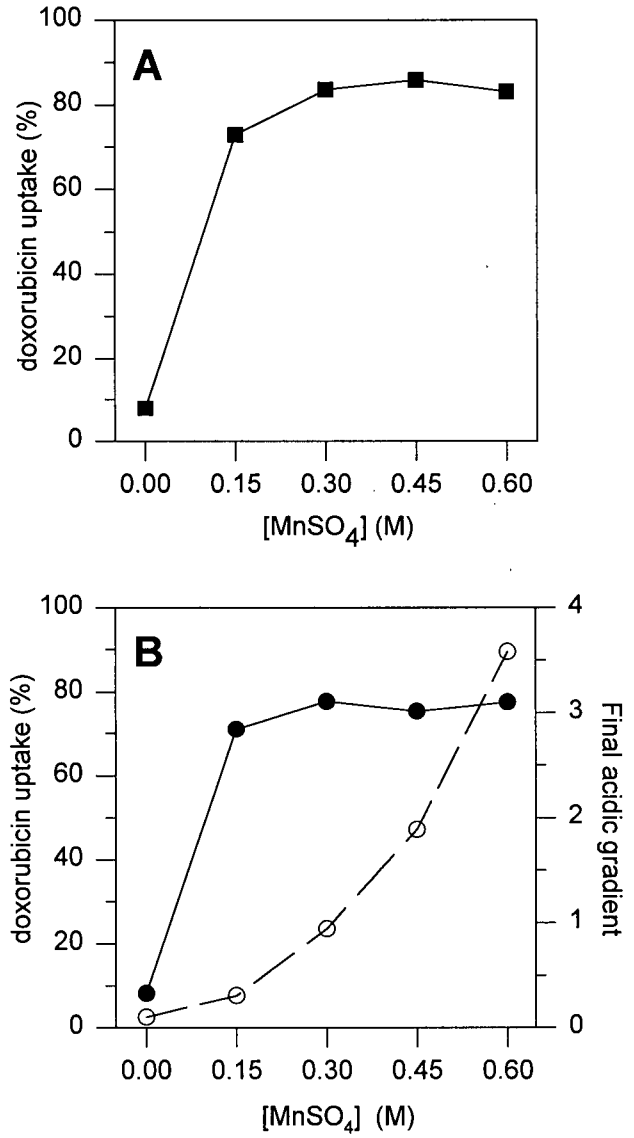

Figure 16. Effects of the intraliposomal $MnSO_4$ concentration on doxorubicin uptake. (A) shows the % doxorubicin uptake achieved in the absence of A23187. (B) shows the effects of intraliposomal $MnSO_4$ concentration on doxorubicin uptake (●) and on the final acidic gradient (○) in the presence of A23187. Doxorubicin uptake and the final acidic gradient were determined after their readings became constant (60 to 120 min). All concentrations of $MnSO_4$ solutions were titrated to and buffered at pH 7.4 with 30 mM Hepes. When no $MnSO_4$ was present (0 M), the LUVs contained 0.30 M Na_2SO_4 and 30 mM Hepes (pH 7.4). Uptake in both panels was performed at a drug-to-lipid molar ratio of 1.0 at 60 °C.

2.3.6 The pH of the entrapped $MnSO_4$ solution has minimal effect on doxorubicin uptake

In order to simplify data interpretation, we employed entrapped pH 7.4 $MnSO_4$ solution to eliminate any contributions of an initial pH gradient to the doxorubicin uptake in the Mn^{2+}-containing system. To test whether liposomes with unbuffered $MnSO_4$ (pH 4.0) could be used for doxorubicin loading instead of the titrated $MnSO_4$ solution at pH 7.4, doxorubicin uptake into liposomes containing $MnSO_4$ encapsulated at pH 4.0 or at pH 7.4 were performed and the results are illustrated in Figure 17. In the absence of A23187, there is no significant difference in the drug loading effectiveness between the pH 4.0 and the pH 7.4 $MnSO_4$-entrapped liposomes.

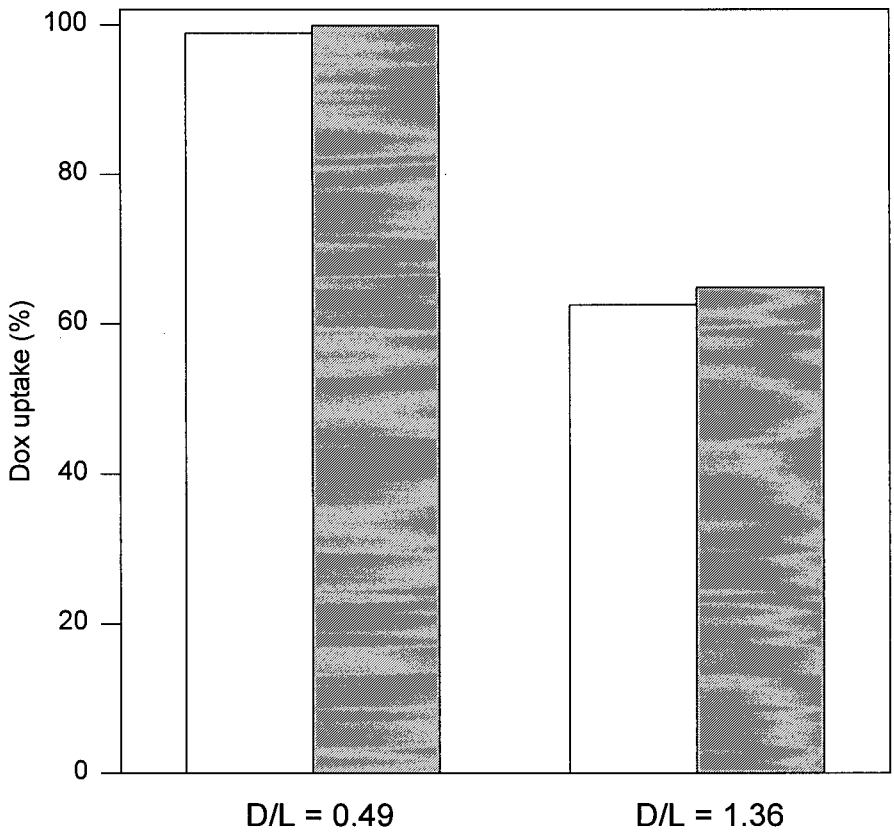

Figure 17. Effect of pH of the encapsulated $MnSO_4$ on doxorubicin uptake in the absence of A23187. Encapsulated $MnSO_4$ solutions were either untitrated (pH 4.0, ▓) or titrated with 30 mM Hepes (pH 7.4, □). The drug-to-lipid molar ratios administered were 0.49 and 1.36.

2.3.7 Doxorubicin is stably entrapped after accumulation in response to a Mn^{2+} gradient

To assess the stability of the liposomal doxorubicin systems, *in vitro* leakage assays were performed employing 50 % (v/v) mouse serum. Doxorubicin was loaded in the presence or absence of A23187 at a drug-to-lipid molar ratio of 0.5. After removing unencapsulated doxorubicin, the liposomes loaded with doxorubicin were diluted with mouse serum and incubated at 37 °C for 24 h. The final lipid concentration in 50 % mouse serum was 1 mM. Figure 18 shows that virtually no drug leakage was observed over a 24 h period for Mn^{2+}-containing LUVs loaded in the presence or absence of A23187.

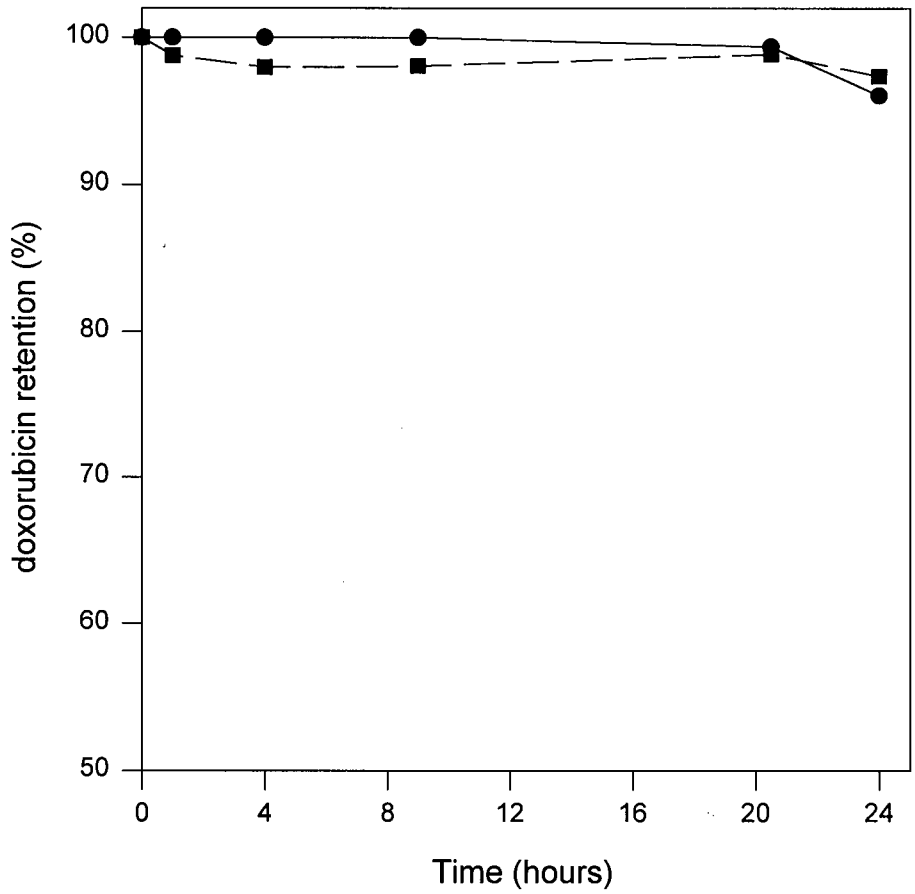

Figure 18. In vitro leakage assay of liposomal doxorubicin using 50 % mouse serum. Liposomal doxorubicin was loaded at a drug-to-lipid molar ratio of 0.5 in the presence (●) and the absence (■) of A23187 by incubating doxorubicin with liposomes at 60 °C for 70 min. Subsequently, the liposomal doxorubicin was centrifuged through spin columns before incubating for 24 h with mouse serum at 37 °C. The lipid concentration in the mixture containing 50 % mouse serum during the leakage assay was 1 mM.

Chapter 3
Discussion

The results presented here demonstrate a novel method for the loading of doxorubicin into liposomes. It is shown that doxorubicin uptake can be driven by a transmembrane Mn^{2+} gradient, in the absence of any pH gradient. Loading procedures for doxorubicin described previously all rely on the presence of a transmembrane pH gradient to drive uptake (Culllis et al., 1997). Loading of doxorubicin in response to a transmembrane Mn^{2+} gradient relies on the formation of a membrane-impermeable complex with Mn^{2+}. In this section, we discuss the mechanism, properties, and potential applications of this loading procedure.

The formation of doxorubicin-Mn^{2+} complexes with a high stability constant (pK_D = 7.0) has been previously described (Bouma et al., 1986). Complex formation is accompanied by the changes in the absorption spectrum of doxorubicin upon titrating with Mn^{2+} (Figure 14A), which changes the colour of doxorubicin from red to purple. This colour change is also observed during doxorubicin loading into the liposomes in response to a Mn^{2+} gradient in both the presence and absence of A23187. In the presence of the ionophore A23187, however, the colour changes back to red after the doxorubicin is loaded, indicating dissociation of the doxorubicin-Mn^{2+} complex after re-establishment of the pH gradient (inside acidic) by the ionophore. This was confirmed by the absorption spectrum of the liposomal doxorubicin that was loaded in the presence of A23187 (Figure 14D), which is characteristic of protonated doxorubicin. The absorption spectrum of liposomal doxorubicin loaded in the absence of ionophore is red-shifted, indicating the formation of complexes with Mn^{2+}.

For Cu^{2+}, it has been reported that two doxorubicin molecules complex with one Cu^{2+} ion at pH 7.4 (Greenaway and Dabrowiak, 1982), and one proton is released from the aglycone portion of each doxorubicin molecule (Bouma et al., 1986). Complex formation only occurs when the sugar amine of doxorubicin is neutral (Lenkinski et al., 1983). Assuming that similar behaviour is observed for Mn^{2+}, a model for doxorubicin complexation with Mn^{2+} is suggested in Figure 19.

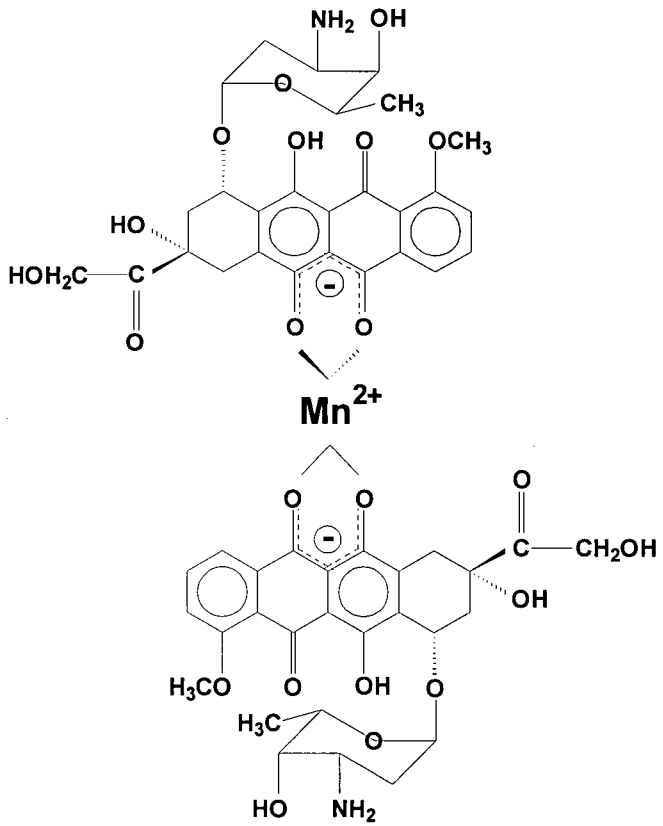

Figure 19. Chemical structure of doxorubicin-Mn^{2+} complex

Upon loading of doxorubicin into Mn^{2+}-containing liposomes, complexation of two doxorubicin molecules with one Mn^{2+} ion will release two protons, thereby acidifying the intraliposomal medium. This will result in the protonation of the next two doxorubicin molecules that enter the liposome interior. From the overall doxorubicin uptake scheme outlined in Figure 20, the addition of doxorubicin would equalize the pH_i to the pH_o, as was found in experiments where the external pH was varied (data not shown). As long as $pH_i < pH_o$, doxorubicin that enters the liposome interior will be protonated; protonation of doxorubicin depletes the intraliposomal protons and raises the pH_i. This protonation process provides the driving force for doxorubicin uptake until $pH_i = pH_o$. After that, uptake will take place by alternating between Mn^{2+} complexation and protonation as given in Figure 20. In the opposite case, when $pH_i > pH_o$ initially, doxorubicin that enters the liposome interior will complex with Mn^{2+}. This will result in the release of protons from the aglycone region, which decreases the pH_i until $pH_i = pH_o$. Subsequently, drug uptake again will take place by alternating between complexation and protonation. In the experiments described in Figure 15, the pH_i was rapidly equalized to the pH_o within the first 5 min of drug loading. Only background levels of doxorubicin uptake were observed at $pH_o = 6.5$ or lower, and drug uptake increases at higher pH_o (Figure 15). This can be explained by the fact that doxorubicin-Mn^{2+} complexation is pH dependent (Bouma et al., 1986; Figure 3B) as the pH_o equals to the pH_i within 5 min of drug uptake. Half of the maximum level of doxorubicin uptake occurs at about pH 7.0, close to the pK_a of the saturating doxorubicin-Mn^{2+} complex ($pK_a = 6.6$; Figure 14C).

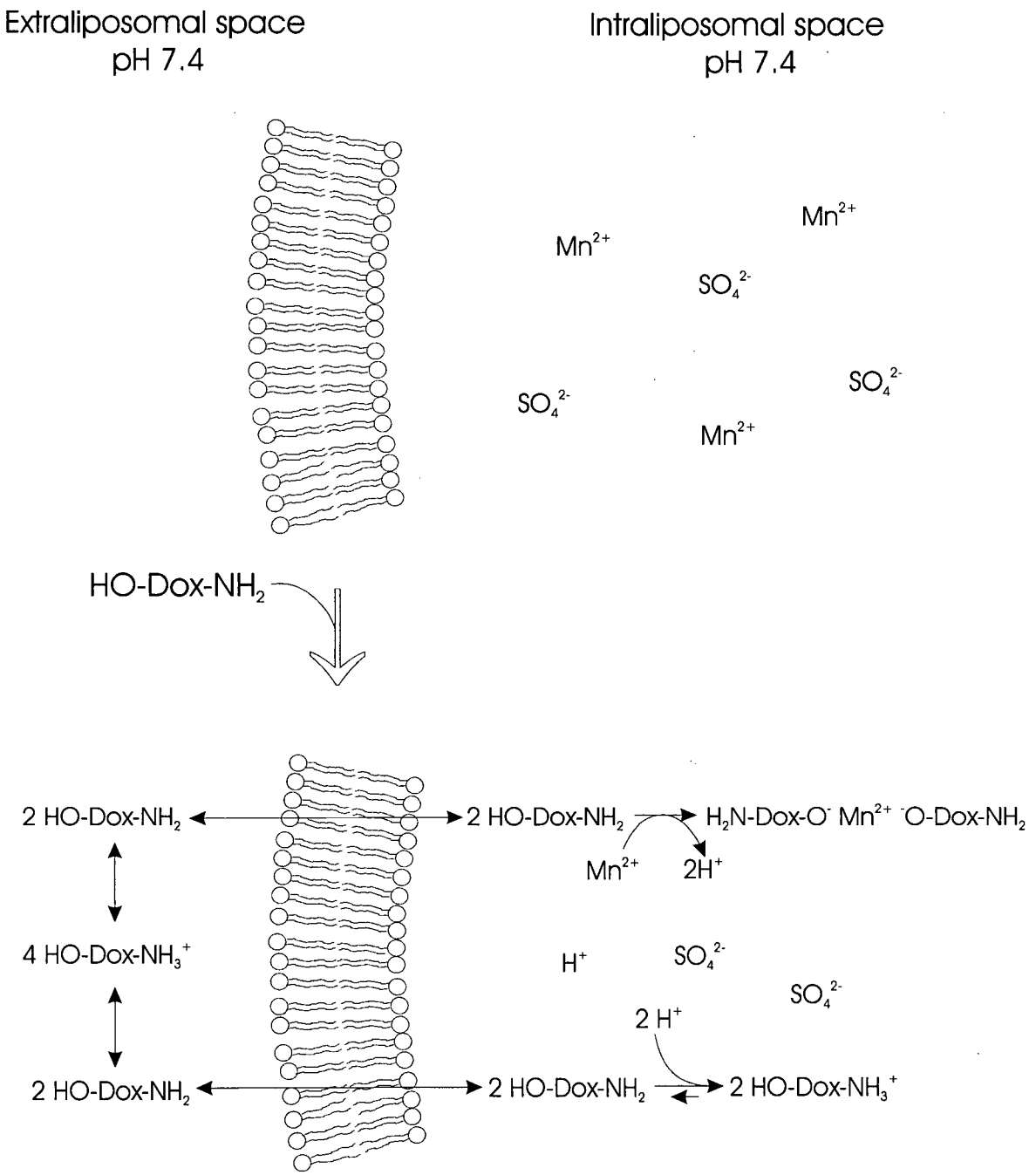

Figure 20. Schematic representation of reactions involved in the loading of doxorubicin (Dox) in response to a transmembrane Mn^{2+} gradient. The hydroxyl (-OH) group attached to the "Dox" molecule is on the anthraquinone moiety of doxorubicin; the amine ($-NH_2$ or $-NH_3^+$) group attached to the "Dox" molecule corresponds to the amine on the sugar moiety.

The discrepancy between the apparent pK_a (6.6) and the pH for half-maximal (7.0) uptake may be due to the fact that the intraliposomal Mn^{2+} concentration is not sufficient to saturate the doxorubicin inside the liposomes. As demonstrated in Figure 14A, 50 mM $MnSO_4$ is required to half-saturate 54 μM doxorubicin. Assuming a trapped volume of 1.5 μL/μmol lipid for 100 nm LUVs (Hope et al., 1985; Veiro and Cullis, 1990) and using a drug-to-lipid molar ratio of 1.0, the concentration of doxorubicin inside the liposomes will be approximately 0.5 M (80% drug uptake; Figure 13). It is apparent that the 0.30 M Mn^{2+} inside the liposomes cannot saturate the 0.5 M liposomal doxorubicin. Consequently, the pK_a of the doxorubicin sugar amine will be lowered to below 8.15 due to the presence of Mn^{2+}, but not as low as 6.6 which is obtained only in the presence of saturating concentrations of Mn^{2+}.

Under the appropriate experimental conditions, doxorubicin loading in response to a transmembrane Mn^{2+} gradient is very efficient. Uptake levels of 100% can be reached up to a drug-to-lipid molar ratio of 0.5 (Figure 13). When starting with a higher drug-to-lipid molar ratio (1.1), doxorubicin can even be loaded up to a final drug-to-lipid molar ratio of 0.8 (73% uptake). Overall, the efficiency of this loading procedure is comparable to that of the A23187 pH gradient loading method.

Complexation of doxorubicin with several metal ions (such as Fe^{3+} and Cu^{2+}) has been reported to facilitate the binding of the anthracycline to DNA, promote the peroxidation of lipids, and enhance the generation of reactive oxygen species (Bachur et al., 1977; Bouma et al., 1986; Gutteridge, 1984; Lown et al., 1982; Muindi et al., 1984). These actions inside cells promote cell death through damaging intracellular organelles. For doxorubicin-Fe^{3+} and doxorubicin-Cu^{2+} complexes, enhanced cytotoxicity has been

described (Gutteridge, 1984; Muindi et al., 1984; Hasinoff, 1989; Greenaway and Dabrowiak, 1982; Hasinoff et al., 1989). Therefore, a liposomal formulation of doxorubicin-Mn^{2+} complex could be therapeutically advantageous. In this regard, a concentration of $MnSO_4$ (0.30 M) iso-osmotic to physiological saline solution was employed and was found to be sufficient to drive a high level of doxorubicin uptake at drug-to-lipid molar ratios as high as 1.0. Doxorubicin loaded by a transmembrane Mn^{2+} gradient through the formation of drug-Mn^{2+} complexes has been shown to be active *in vitro* on HEK 293, COS-7 and J774 cells (data not shown). Therefore, doxorubicin is still active against cells after the formation of drug-Mn^{2+} complexes inside liposomes. Finally, *in vitro* leakage assays reveal that doxorubicin loaded in response to entrapped Mn^{2+} exhibits excellent retention over a 24-hour incubation period at 37 °C. These properties suggested that liposomal doxorubicin formulations loaded in response to entrapped $MnSO_4$ may have promise for *in vivo* applications.

Some of the results in this thesis have been presented in Leenhouts et al., 1997

Bibliography

Amselem, S., A. Gabizon, and Y. Barenholz. 1990. Optimization and upscaling of doxorubicin-containing liposomes for clinical use. Journal of Pharmaceutical Sciences. 79: 1045-1052.

Bachur, N.R., S.L. Gordon, and M.V. Gee. 1977. Anthracycline antibiotic augmentation of microsomal electron transport and free radical formation. Molec. Pharmac. 13 (5): 901-910.

Barenholz, Y., S. Amselem, and D. Lichtenberg. 1979. A new method for preparation of phospholipid vesicles (liposomes)-French Press. FEBS Letters. 99: 210-214.

Bally, M.B., R. Nayar, D. Masin, P.R. Cullis, and L.D. Mayer. 1990. Studies on the myelosuppressive activity of doxorubicin entrapped in liposomes. Cancer Chemother. Pharmacol. 27 (1): 13-19.

Benjamin, R.S. 1975. A practical approach to adriamycin (NSC-123127) toxicology. Cancer Chemother. Rep. 6: 191-198.

Blum, R.H., and S.K. Carter. 1974. Adriamycin: a new anticancer drug with significant clinical activity. Ann. Intern. Med. 80: 245-259.

Bouma, J., J.H. Beijnen, A. Bult, and W.J.M. Underberg. 1986. Anthracycline antitumour agents: A review of physiochemical, analytical and stability properties. Pharmaceutisch Weekblad Scientific Edition. 8: 109-133.

Chapman, C.J., A.K. Puri, R.W. Taylor, and D.R. Pfeiffer. 1987. Equilibria between ionophore A23187 and divalent cations: stability of 1:1 complexes in solutions of 80% methanol/water. Biochemistry. 26: 5009-5018.

Crommelin, D.J.A., and L. von Bloois. 1983. Preparation and characterization of doxorubicin containing liposomes. Part 2. Loading capacity, long term stability and doxorubicin bilayer interaction mechanism. International Journal of Pharmaceutics. 17: 135-144.

Cullis, P.R., M.J. Hope, M.B Bally, T.D. Madden, L.D. Mayer, and D.B. Fenske. 1997. Influence of pH gradients on the transbilayer transport of drugs, lipids, peptides and metal ions into large unilamellar vesicles. Biochim. Biophys. Acta. 1331: 187-211.

Cullis, P.R., B. de Kruijff, M.J. Hope, A.J. Verkleij, R. Nayer, S.B. Farren, C. Tilcock, T.D. Madden, and M.B. Bally. 1983. Structural properties of lipids and their functional roles in biological membranes. Membrane Fluidity in Biology (R.C. Aloia Ed.), vol. 1, pp. 39-81. Academic Press, New York.

Daemen, T., J. Regts, M. Meesters, M.T.T. Kate, I.A.J.M. Bakker-Woudenberg, and G.L. Scherphof. 1997. Toxicity of doxorubicin entrapped with long-circulating liposomes. J. Controlled Release. 44: 1-9.

De Wolf, F.A., R.W.H.M. Staffhorst, H. Smits, M.F. Onwezen, and B. de Kruijff. 1993. Role of anionic phospholipids in the interaction of doxorubicin and plasma membrane vesicles: drug binding and structure consequences in bacterial systems. Biochemistry. 32 (26): 6688-6695.

Estep, T.N., D.B. Mountcastle, Y. Barenholz, R.L. Biltonen, and T.E. Thompson. 1979. Thermal behavior of synthetic sphingomyelin-cholesterol dispersions. Biochemistry. 18 (10): 2112-2117.

Fenske, D.B., Wong, K.F., Maurer, E., Maurer, N., Leenhouts, J.M., Boman, N., Amankwa, L., and Cullis, P.R. 1998. Submitted for publication.

Fiske, C.H., and Y. Subbarow. 1925. The colorimetric determination of phosphorus. J. Biol. Chem. 66: 375-400.

Gabizon A., D. Goren, Z. Fuks, A. Meshorer, and Y. Barenholz. 1985. Superior therapeutic activity of liposome-associated adriamycin in a murine metastatic tumor model. Br. J. Cancer. 51 (5): 681-689.

Gennis, R.B. 1989. Biomembranes: Molecular Structure and Function. Springer-Verlag, New York.

Greenaway, F.T., and J.C. Dabrowiak. 1982. The binding of copper ions to daunomycin and adriamycin. J. Inorg. Biochem. 16: 91-107.

Gutteridge, J.M.C. 1984. Lipid peroxidation and possible hydroxyl radical formation stimulated by the self-reduction of doxorubicin-iron (III) complex. Biochem. Pharmac. 33 (11): 1725-1728.

Haran, G., R. Cohen, L.K. Bar, and Y. Barenholz. 1993. Transmembrane ammonium sulphate gradients in liposomes produce efficient and stable entrapment of amphipathic weak bases. Biochim. Biophys. Acta. 1151: 201-215.

Harrigan, P.R., K.F. Wong, T.E. Redelmeier, J.J. Wheeler, and P.R. Cullis. 1993. Accumulation of doxorubicin and other lipophilic amines into large unilamellar vesicles in response to transmembrane pH gradients. Biochim. Biophys. Acta. 1149 (2): 329-338.

Harrigan, P.R., M.J. Hope, T.E. Redelmeier, and P.R. Cullis. 1992. Determination of transmembrane pH gradients and membrane potentials in liposomes. Biophys. J. 63 (5): 1336-1345.

Hasinoff, B.B. 1989. Self-reduction of the iron(III)-doxorubicin complex. Free Radical Biology & Medicine. 7 (6): 583-593.

Hasinoff, B.B., J.P. Davey, and P.J. O'Brien. 1989. The adriamycin (doxorubicin)-induced inactivation of cytochrome c oxidase depends on the presence of iron or copper. Xenobiotica. 19 (2): 231-241.

Herman, E.H., A. Rahman, V.J. Ferrans, J.A. Vick, and P.S. Schein. 1983. Prevention of chronic doxorubicin cardiotoxicity in beagles by liposomal encapsulation. Cancer Res. 43 (11): 5427-5432.

Hope, M.J., M.B. Bally, G. Webb, and P.R. Cullis. 1985. Production of large unilamellar vesicles by a rapid extrusion procedure. Characterization of size distribution, trapped volume and ability to maintain a membrane potential. Biochim. Biophys. Acta. 812: 55-65.

Huang, C.H. 1969. Studies on phosphatidylcholine vesicles: formation and physical characteristics. Biochemistry. 8: 344-351.

Kulkarni, S.B., G.V. Betageri, and M. Singh. 1995. Factors affecting microencapsulation of drugs in liposomes. J. Microencapsulation. 12 (3): 229-246.

Lasic, D.D., B. Ceh, M.C.A. Stuart, L. Guo, P.M. Frederik, and Y. Barenholz. 1995. Transmembrane gradient driven phase transitions witin vesicles: lessons for drug delivery. Biochim. Biophys. Acta. 1239: 145-156.

Lee, R.J., and P.S. Low. 1995. Folate-mediated tumor cell targeting of liposome-entrapped doxorubicin in vitro. Biochim. Biophys. Acta. 1233 (2): 134-144.

Leenhouts, J.M., B. Cheung, T. Sun, D.B. Fenske, and P.R. Cullis. 1997. New procedures for the loading of doxorubicin into liposomes. FASEB J. 11 (9): A1430.

Lenkinski, R.E., S. Sierke, and M.R. Vist. 1983. Lanthanide complexes of adriamycin. J. Less Common Metals. 94: 359-365.

Lown, J.W., H. Chen, and J.A. Plambeck. 1982. Further studies on the generation of reactive oxygen species from activated anthracyclines and the relationship to cytotoxic action and cardiotoxic effects. Biochem. Pharmacol. 31 (4): 575-581.

Marsh, D. 1990. Handbook of Lipid Bilayers. CRC Press, Florida.

Masood, R., S.R. Husain, A. Rahman, and P. Gill. 1993. Potentiation of Cytotoxicity of Kaposi's Sarcoma related to Immunodeficiency Syndrome (AIDS) by liposome-encapsulated doxorubicin. AIDS Research and Human Retroviruses. 9 (8): 741-746.

Mayer, L.D., M.B. Bally, and P.R. Cullis. 1986. Uptake of adriamycin into large unilamellar vesicles in response to a pH gradient. Biochim. Biophys. Acta. 857 (1): 123-126.

Mayer, L.D., M.B. Bally, P.R. Cullis, S.L. Wilson, and J.T. Emerman. 1990. Comparison of free and liposome encapsulated doxorubicin tumor drug uptake and antitumor efficacy in the SC115 murine mammary tumor. Cancer Letters. 53: 183-190.

Mayer, L.D, T.D. Madden, M.B. Bally, and P.R. Cullis. 1993. pH gradient-mediated drug entrapment in liposomes. In: Liposome Technology (G. Gregoriadis, Ed.) Vol. II: 27.

Mayer, L.D., L.C. Tai, D.S. Ko, D. Masin, R.S. Ginsberg, P.R. Cullis, and M.B. Bally. 1989. Influence of vesicle size, lipid composition, and drug-to-lipid ratio on the biological activity of liposomal doxorubicin in mice. Cancer Res. 49 (21): 5922-5930.

McIntosh, T.J., S.A. Simon, D. Needham, and C-H. Huang. 1992. Structure and cohesive properties of sphingomyelin/cholesterol bilayers. Biochemistry. 31: 2012-2020.

Muindi, J.R.F., B.K. Sinha, L. Gianni, and C.E. Myers. 1984. Hydroxyl radical production and DNA damage induced by anthracycline-iron complex. FEBS Lett. 172 (2): 226-230.

Patel, H.M., N.S. Tuzel, and B.E. Ryman. 1983. Inhibitory effect of cholesterol on the uptake of liposomes by liver and spleen. Biochim. Biophys. Acta. 761 (2): 142-151.

Rahman, A., A. Joher, and J.R. Neefe. 1986. Immunotoxicity of multiple dosing regimens of free doxorubicin and doxorubicin entrapped in cardiolipin liposomes. Br. J. Cancer 54 (3): 401-408.

Rahman, A., A. Kessler, N. More, B. Sikic, E. Rowden, P. Woolley, and P.S. Schein. 1980. Liposomal protection of adriamycin-induced cardiotoxicity in mice. Cancer Res. 40 (5): 1532-1537.

Rottenberg, H. 1979. The measurement of membrane potential and delta pH in cells, organelles, and vesicles. Methods Enzymol. 55: 547-569.

Semple, S.C., A. Chonn, and P.R. Cullis. 1996. Influence of cholesterol on the association of plasma proteins with liposomes. Biochemistry. 35 (8): 2521-2525.

Stamp, D., and R.L. Juliano. 1979. Factors affecting the encapsulation of drugs within liposomes. Canadian Journal of Physiology and Pharmacology. 57: 535-539.

Szoka, F.C. 1991. Liposome drug delivery. In: Membrane Fusion. Wilschut J., Hoekston R. (eds). Marcel Dekker: New York: 845-890.

Szoka, F.C., and D. Papahadjopoulos. 1980. Comparative properties and methods of preparation of lipid vesicles (liposomes). Annual Review of Biophysics and Bioengineering. 9: 467-508.

Vaage, J., D. Donovan, P. Uster, and P. Working. 1997. Tumour uptake of doxorubicin polyethylene glycol-coated liposomes and therapeutic effect against a xenografted human pancreatic carcinoma. Br. J. Cancer. 75 (4): 482-486.

Veiro, J.A., and P.R. Cullis. 1990. A novel method for the efficient entrapment of calcium in large unilamellar phospholipid vesicles. Biochim. Biophys. Acta. 1025 (1): 109-115.

Webb, M.S., T.O. Harasym, D. Masin, M.B. Bally and L.D. Mayer. 1995. Sphingomyelin-cholesterol liposomes significantly enhance the pharmacokinetics and therapeutic properties of vincristine in murine and human tumour models. Br. J. Cancer 72 (4): 896-904.